High-speed spray formation probed by Synchrotron X-ray

Nathanaël Machicoane[1], Santanu K. Sahoo[1], Oliver Tolfts[1], and Alexander Rack[2]
[1]*Univ. Grenoble Alpes, CNRS, Grenoble INP, LEGI, 38000 Grenoble, France*
[2]*ESRF - The European Synchrotron, 38000 Grenoble, France*

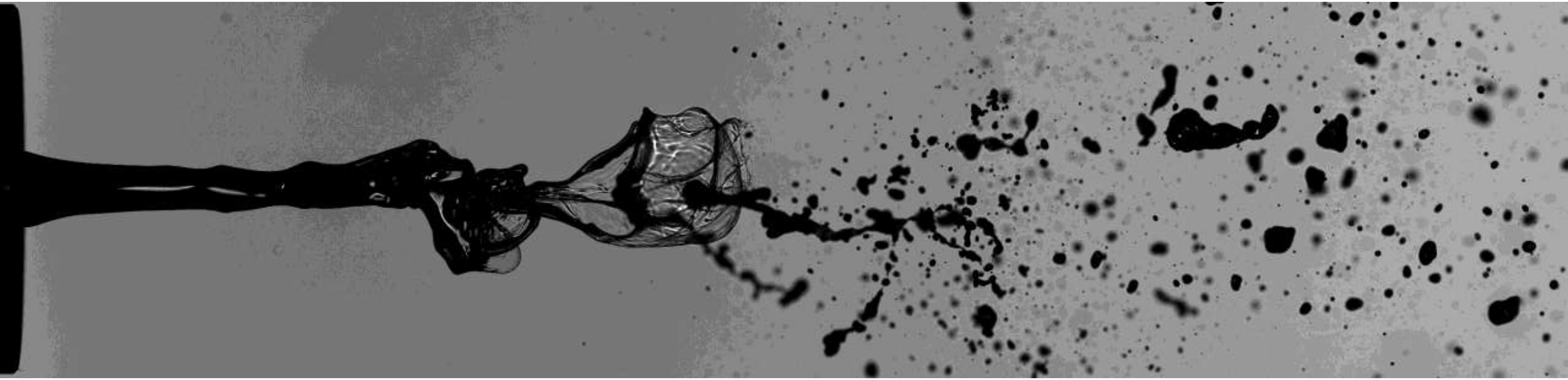

Atomization

- Liquid-gas flows are critical in engineering process innovation and intensification
- Liquid sprays are critical for combustion systems, manufacturing, heat management, chemical processing, painting, e. g.:
  - Liquid fuel sprays
  - Liquid metal atomization
  - Spray cooling and coating
  - Pharmaceutical, food, consumer products
  - Fire safety
  - Ship wake and sea spray


C. Edwards, Stanford University


Fe-Cr ODS Alloy at ~1800 C
I. Anderson, Ames Lab.

Gas-assisted Atomization Phenomena

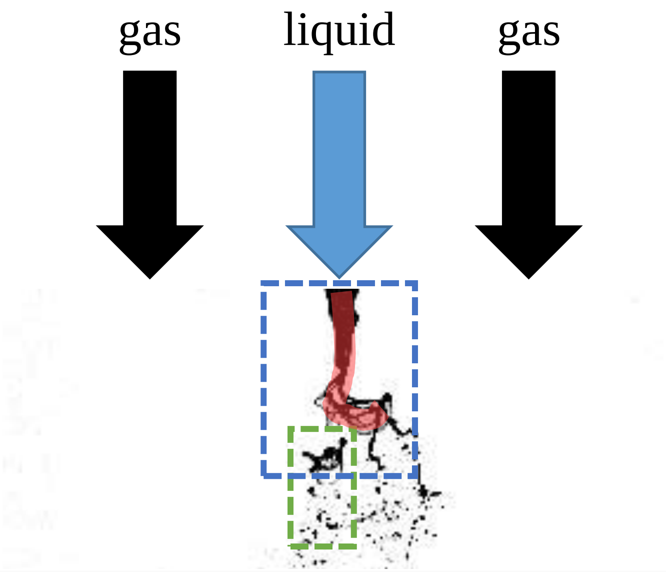

Near field

Gas-assisted atomization: breaking of a liquid jet into a spray (droplet cloud) by a gas co-flow

Spray formation:

- Interfacial instabilities
- Primary break-up

Multiscale process

Large-scale:
FLAPPING

Farago & Chigier, 1992

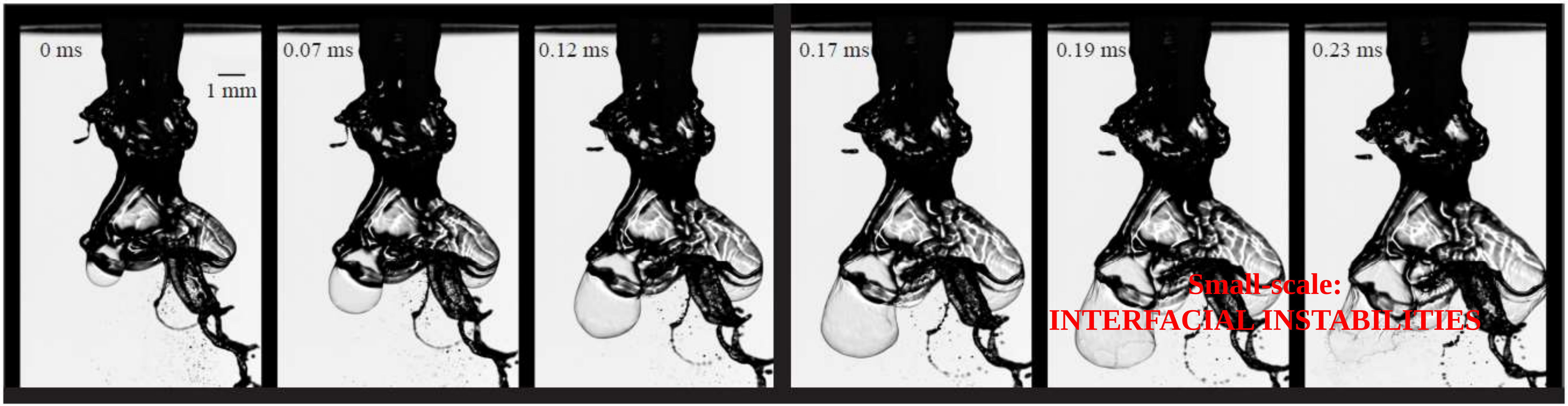

Small-scale:
INTERFACIAL INSTABILITIES

Atomization Physics: Proposed Interfacial Instabilities

Interface destabilized by **surface tension**

Rayleigh–Plateau instability

Interface aligned with **shear**

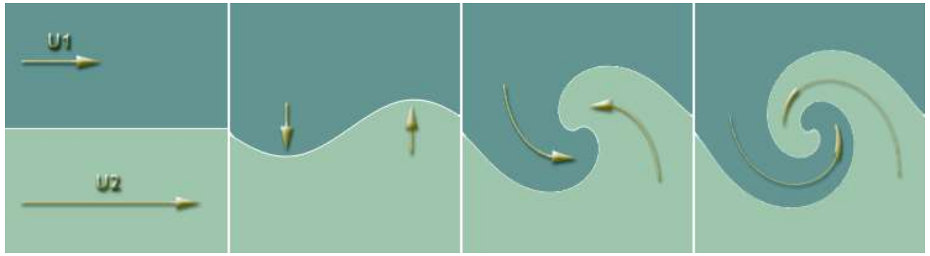

Shear or Kelvin–Helmholtz instability

Accelerated interface (transverse to shear)

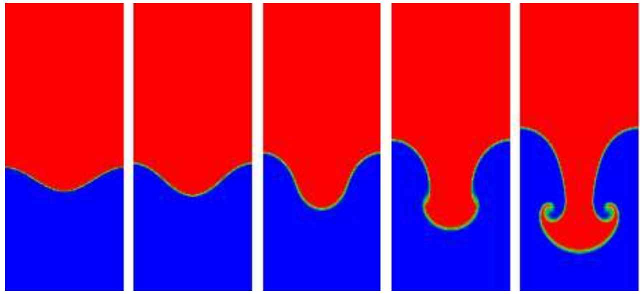

Rayleigh–Taylor instability

Gravity-driven

air

Drop under strong air flow

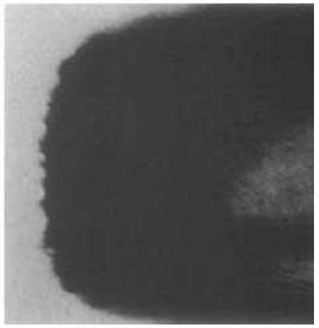

Aero-driven

Drop Break-Up

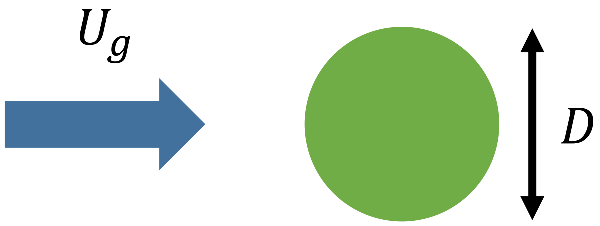

$$We = \frac{\text{gas} - \text{induced stresses}}{\text{surface tension}}$$

$$We = \frac{\rho_g U_g^2 D}{\sigma}$$

Low to moderate Weber numbers

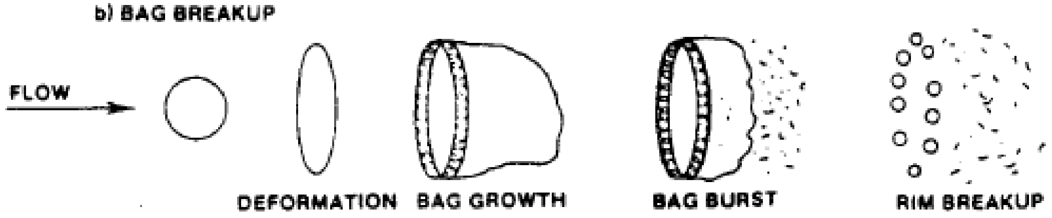

High Weber numbers

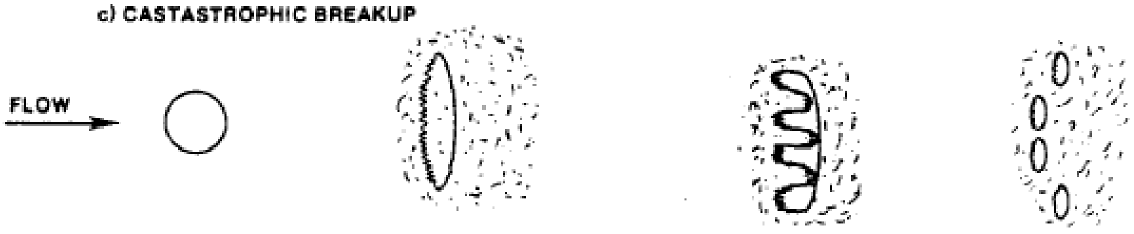

Pilch and Erdman, IJMF 1987

Bag Break-Up

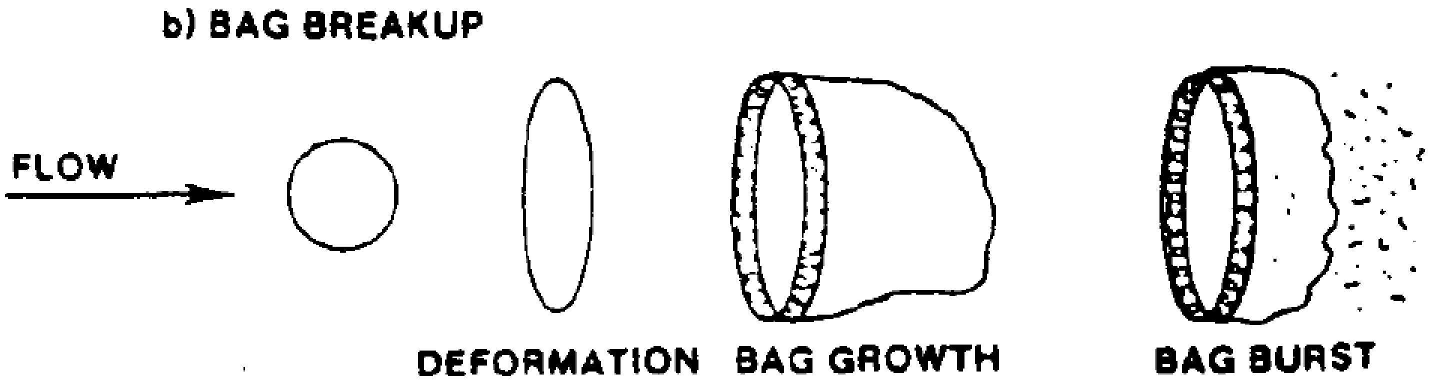
b) BAG BREAKUP
FLOW
DEFORMATION
BAG GROWTH
BAG BURST
RIM BREAKUP

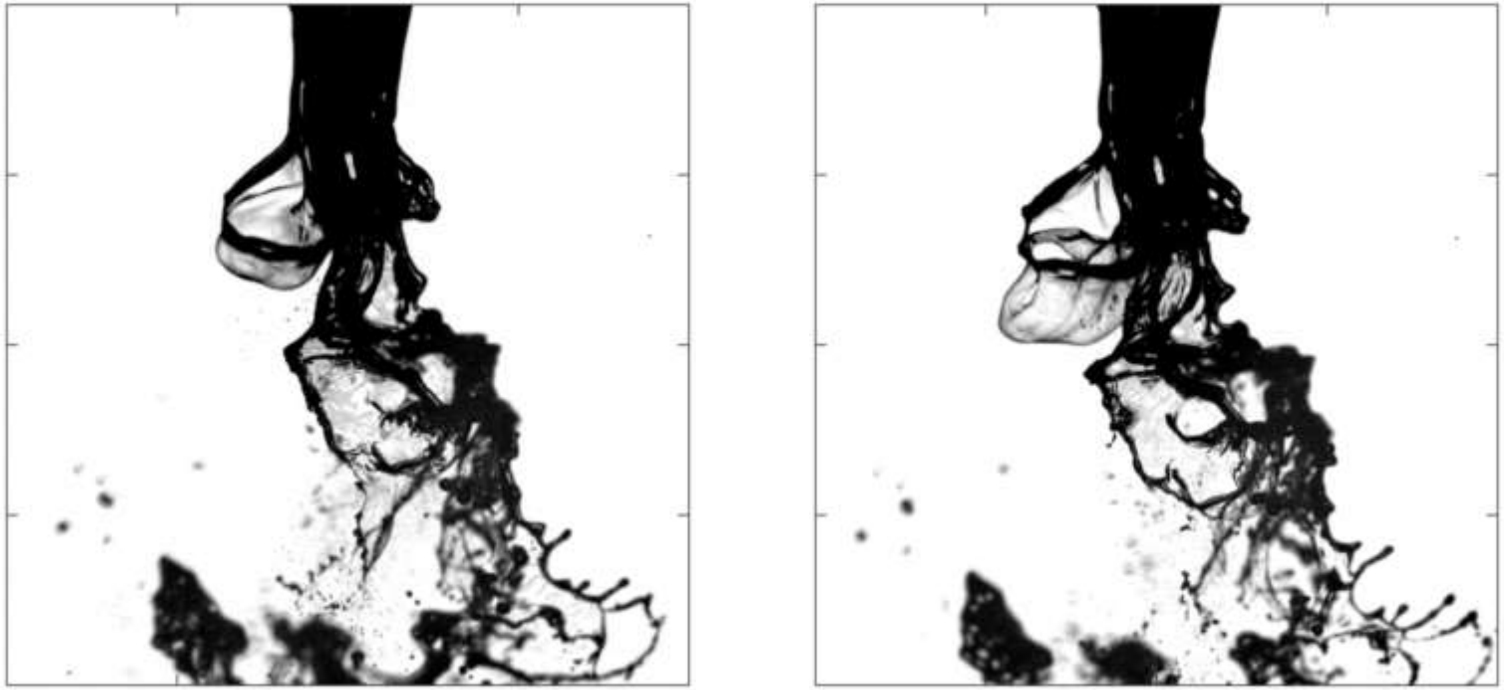


Gas
Liquid
Gas

Fiber-Type Atomization

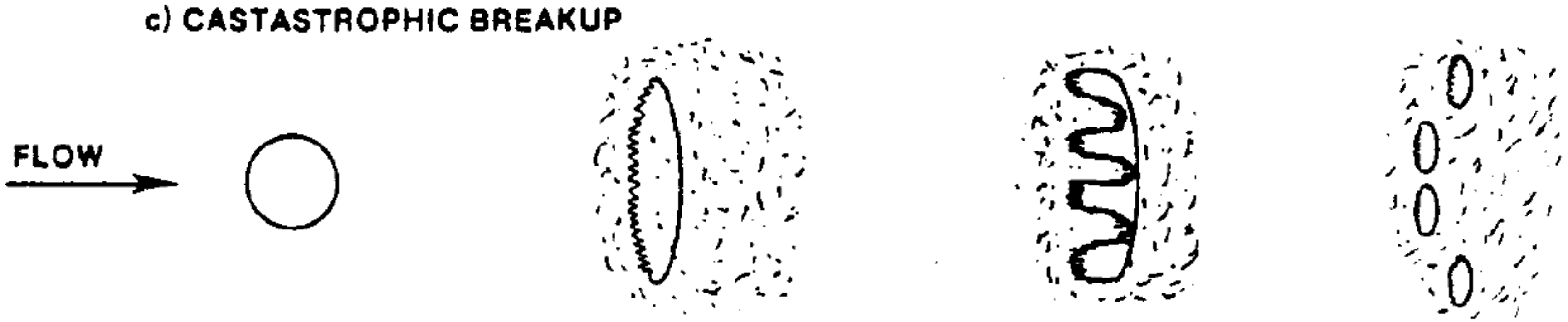

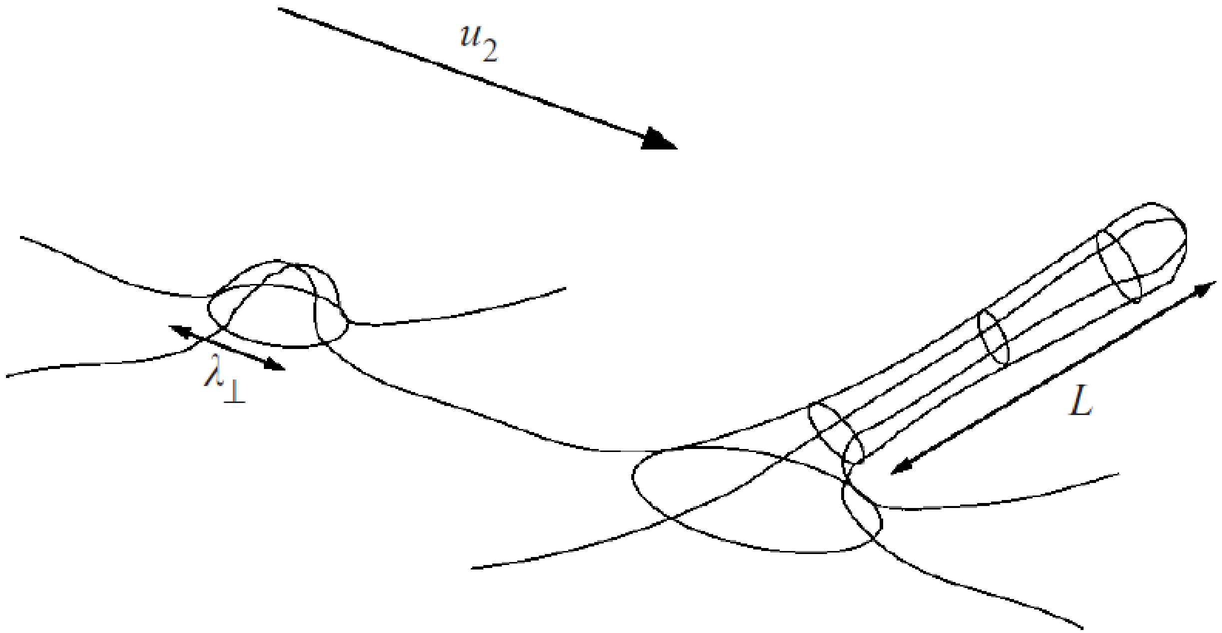

P. Marmottant and E. Villermaux, JFM 2004

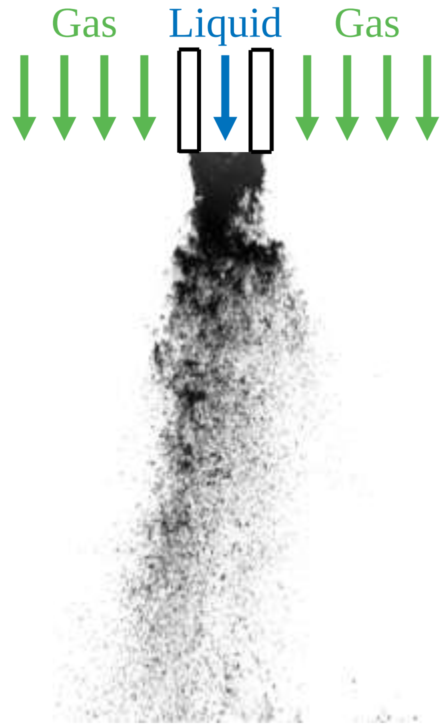

Atomization Regimes

Reynolds and Weber numbers based on the liquid jet diameter

Rims produce large drops that contain a large portion of the liquid volume
➔ incomplete combustion/pollutants

Lasheras & Hopfinger, ARFM 2000

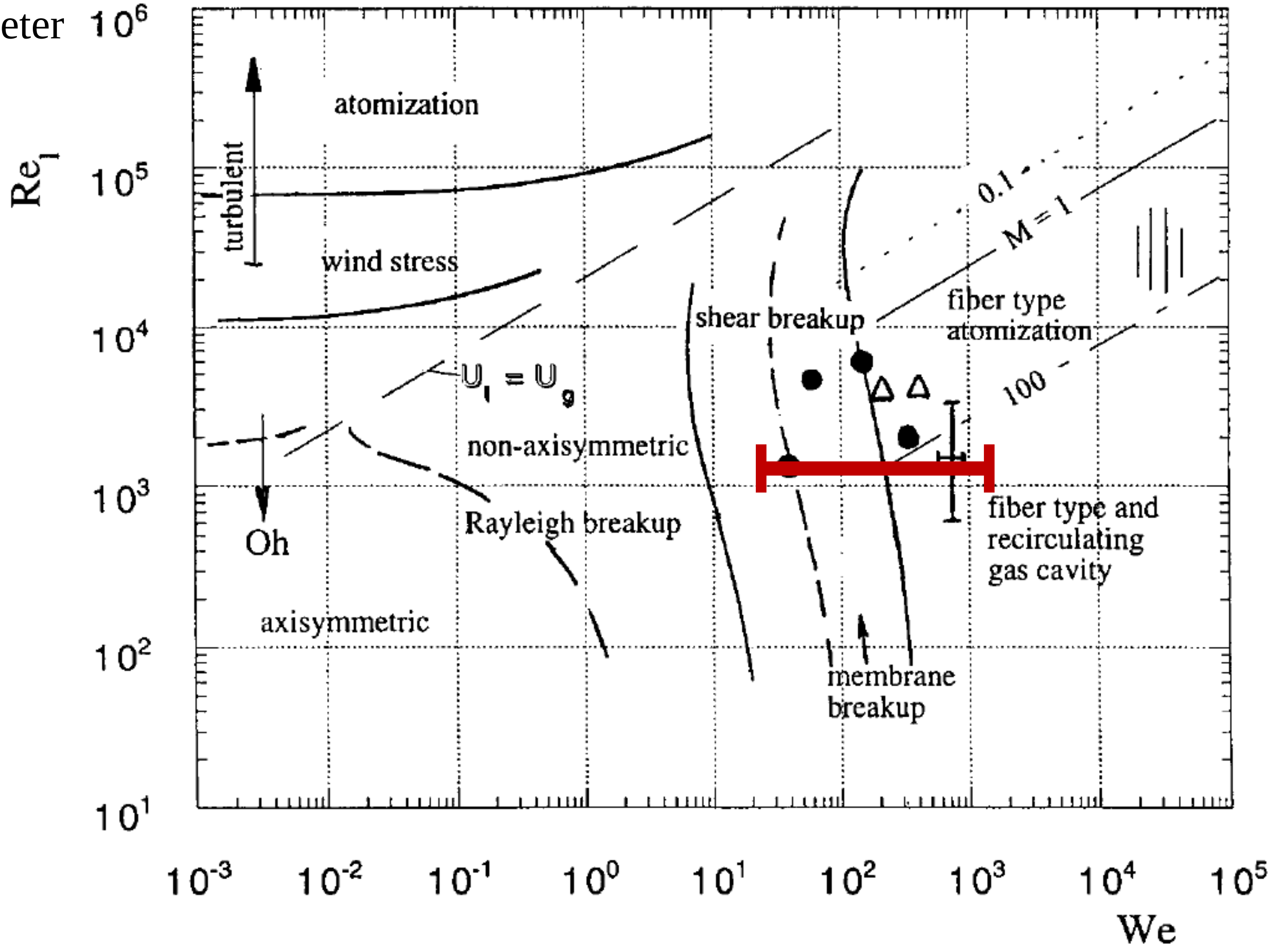

Need for quantitative arguments for change between regimes

Experimental set-up

$700 < \boxed{Re_l} < 20\,000$

$10^4 < Re_g < 10^5$

By varying the gas and liquid flow rates

Weber number

$$\boxed{We_g} = \frac{\rho_g {u_g}^2 d_l}{\sigma}$$

Gas-to-liquid dynamic pressure ratio

$$M = \frac{\rho_g u_g^2}{\rho_l u_l^2}$$

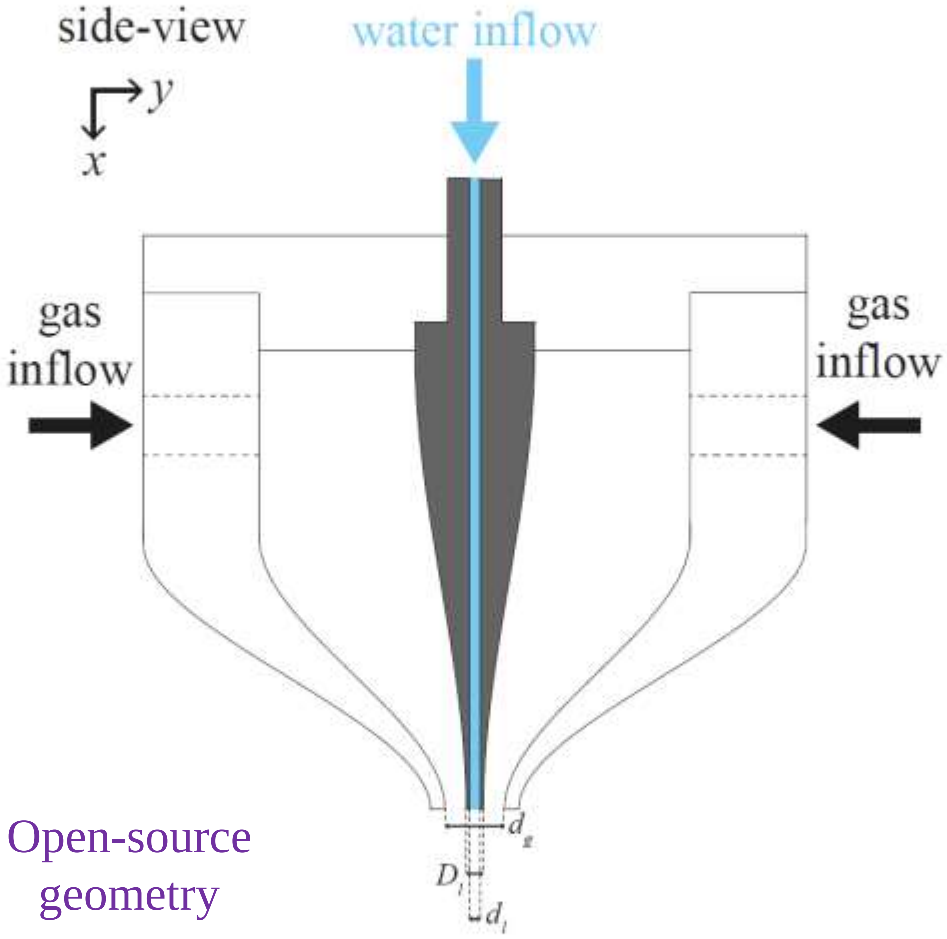

Open-source geometry

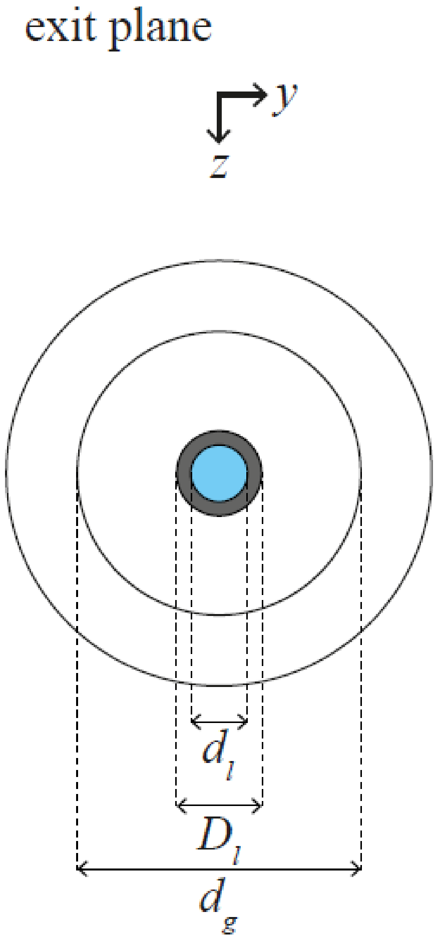

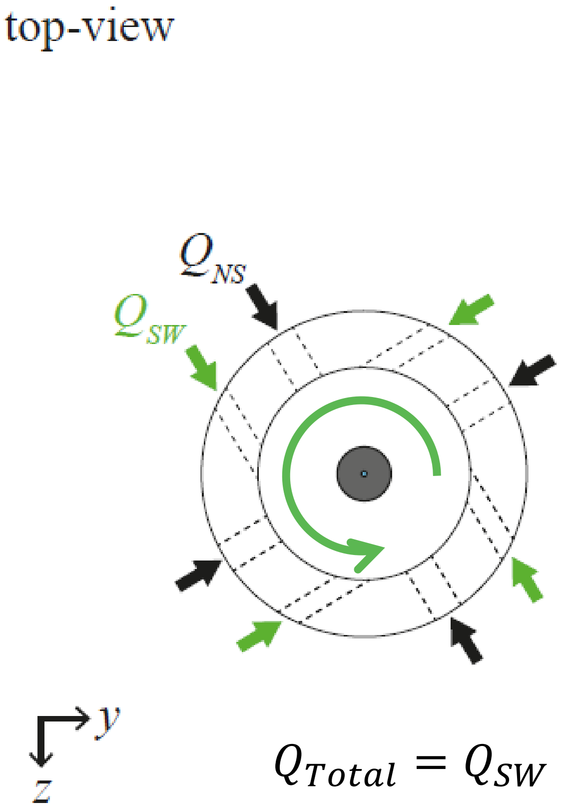

$$Q_{Total} = Q_{SW} + Q_{NS} = cst$$

$$\boxed{SR} = \frac{Q_{swirl}}{Q_{no\ swirl}}$$

Statistics and temporal dynamics of the liquid core length

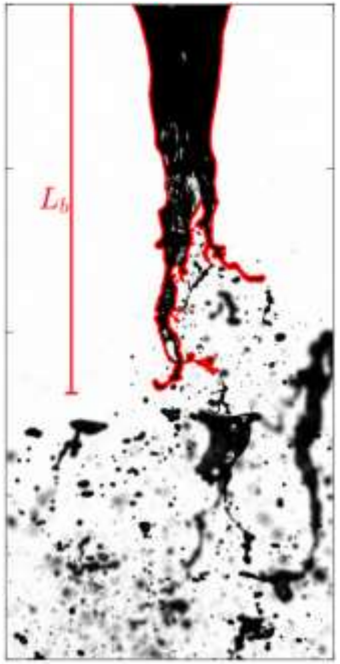

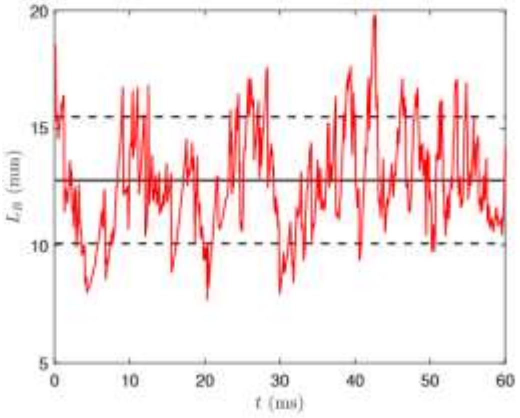

$$\widetilde{L_B} = \frac{L_B - < L_B >}{\mathrm{L_{B,STD}}}$$

- Statistics
- Temporal dynamic

$$R_{L_B}(\tau) = < \widetilde{L_B}(\mathrm{t})\ \widetilde{L_B}(t+\tau) >$$

Liquid

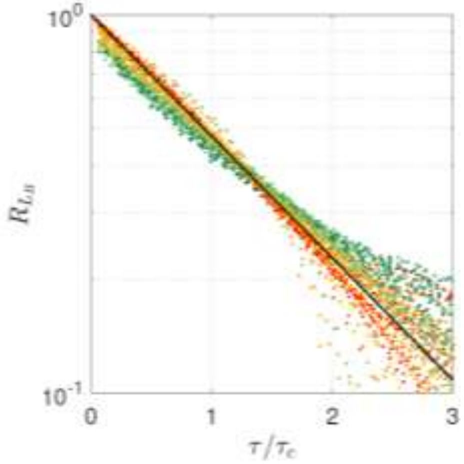

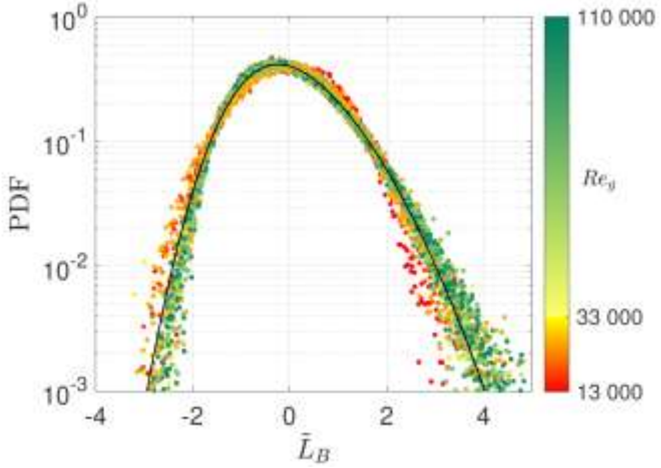

$$\boldsymbol{We_g = 75}$$

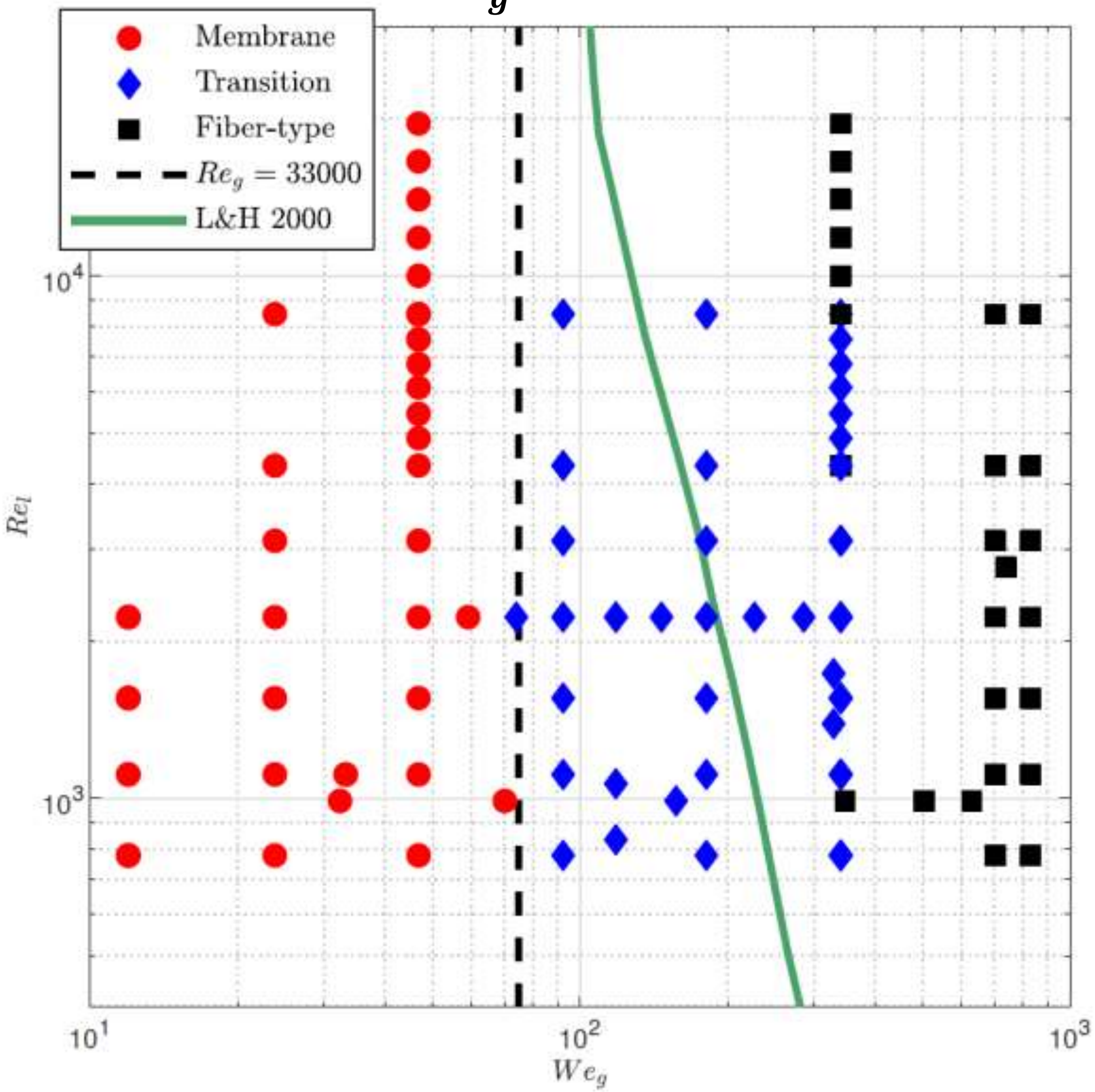

Droplet size distributions in the far-field

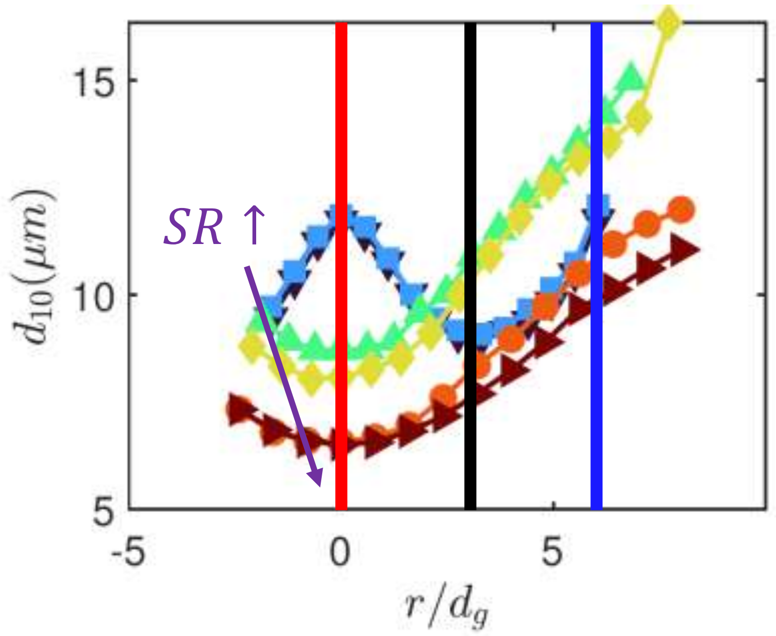

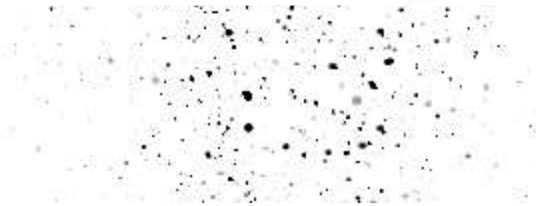

$Re_l = 1100$

$We_g = 850$

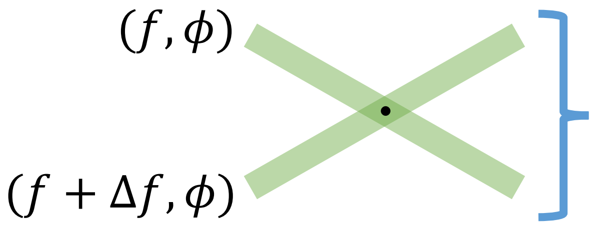

$\Delta\phi$
➔ size

$\Delta f_{Doppler}$
➔ velocity

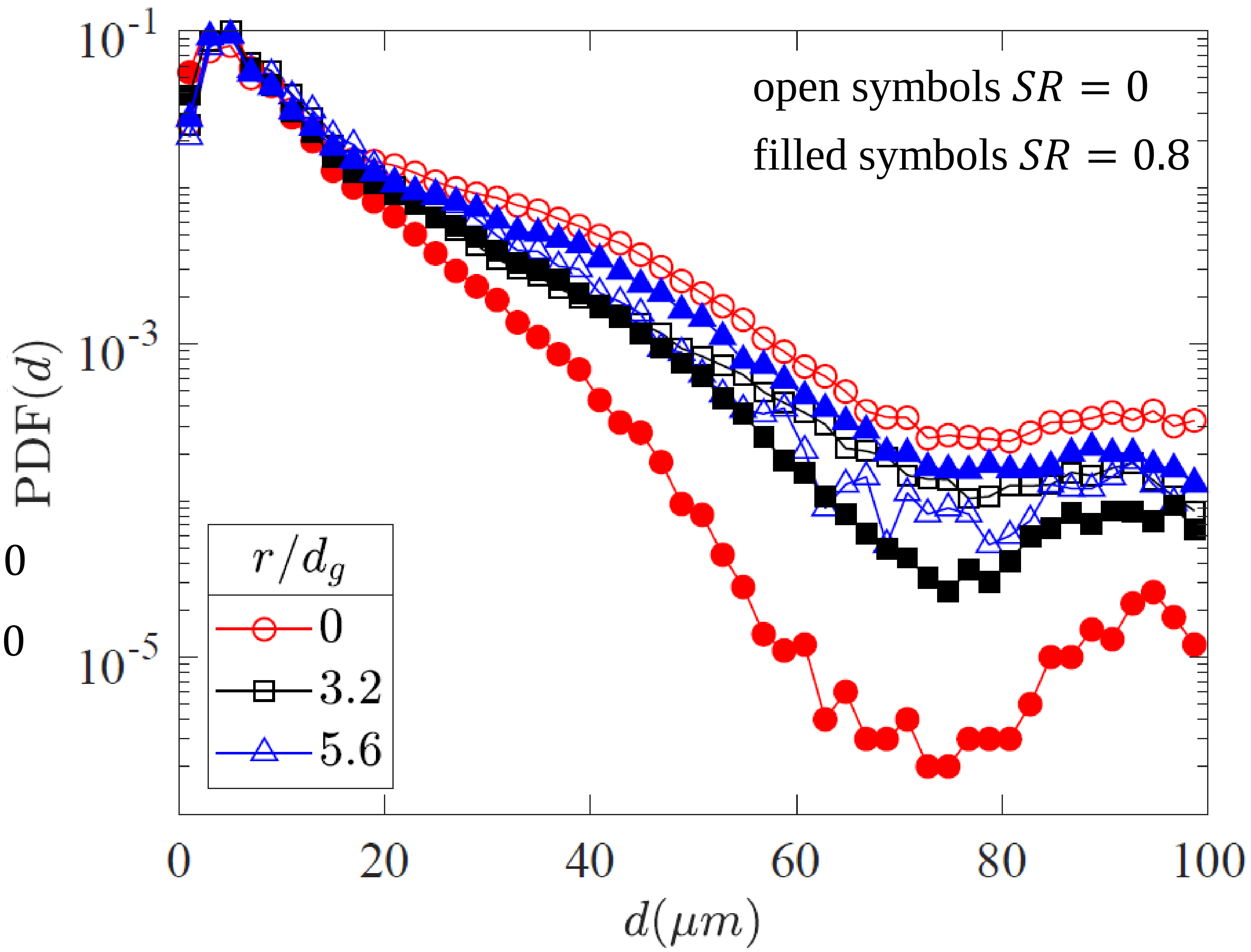

Can we understand the shape of the PDF(d) and how they vary in high-speed spray conditions?

High-speed sprays

A. Rack
ID19

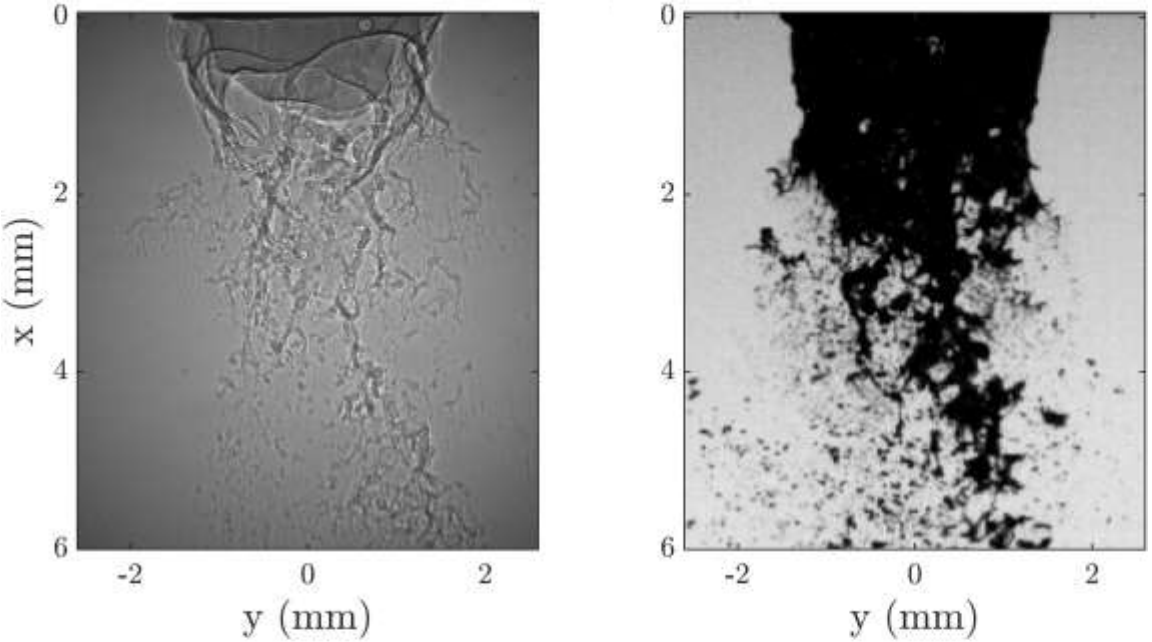

1 s acquisitions
30 – 100 kHz
7 µm per px
Field of view 7x7 mm²

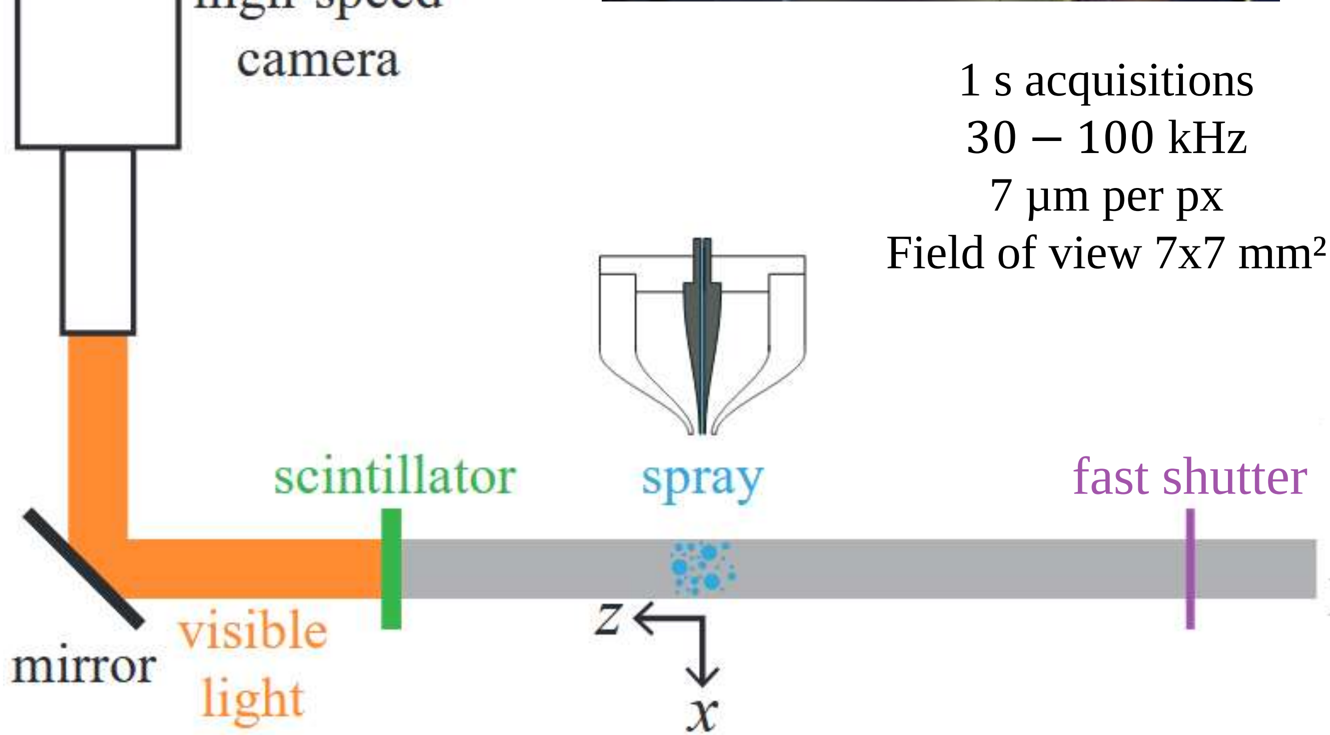

$800 < Re_l < 5000$

$2\,10^4 < Re_g < 2\,10^5$

$30 < We_g < 3200$

$5 < M < 700$

Synchrotron X-ray high-speed imaging

Intact core

$Re_l = 800$ $We_g = 45$

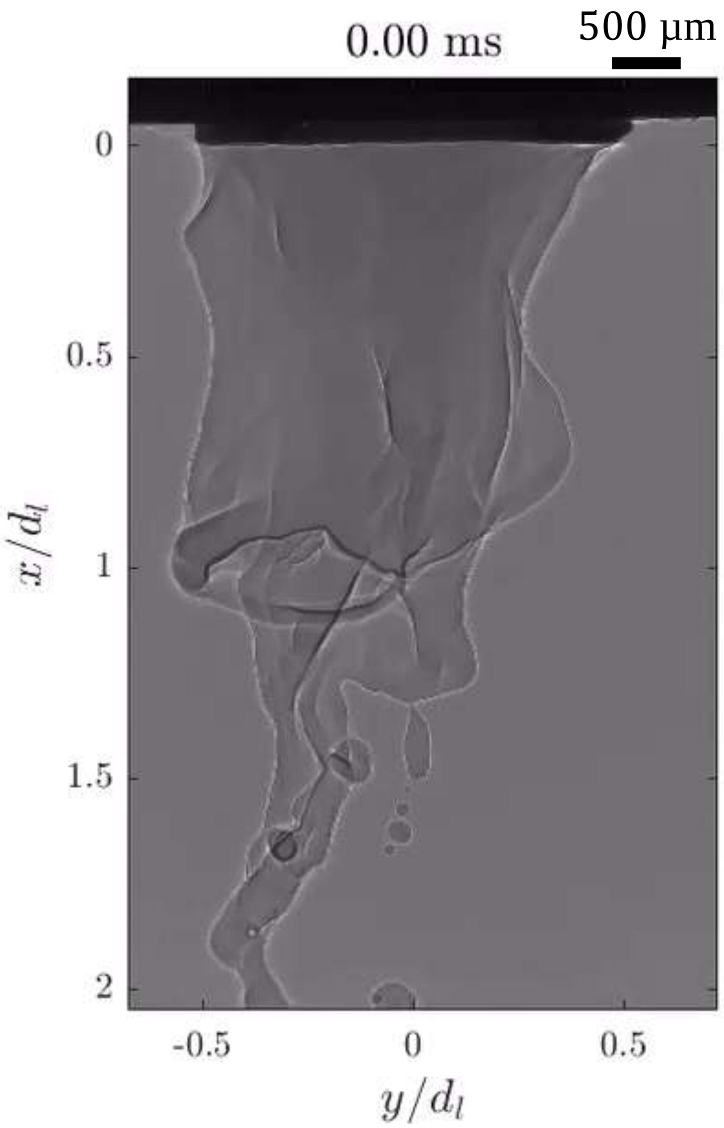

- ➢ No gas penetrated within the liquid jet’s core
- ➢ Strong signature of flapping
- ➢ Formation of bags
- ➢ Localized Kelvin-Helmholtz perturbations
- ➢ Liquid structure reattachments encapsulate large air pockets
- ➢ Full wetting of the liquid nozzle with high curvature as the liquid jet is accelerated

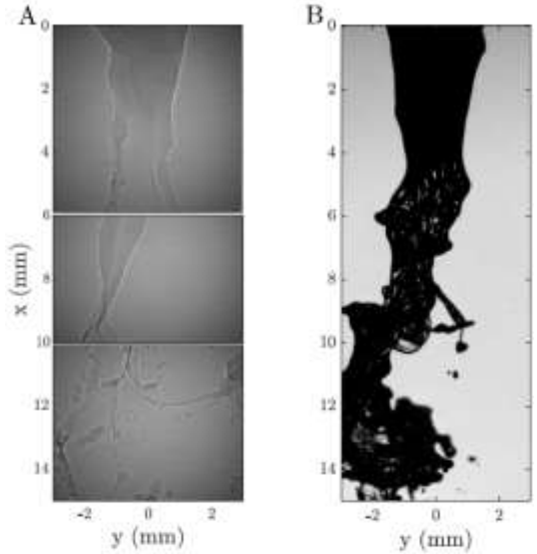

Machicoane et al., IJMF 2019

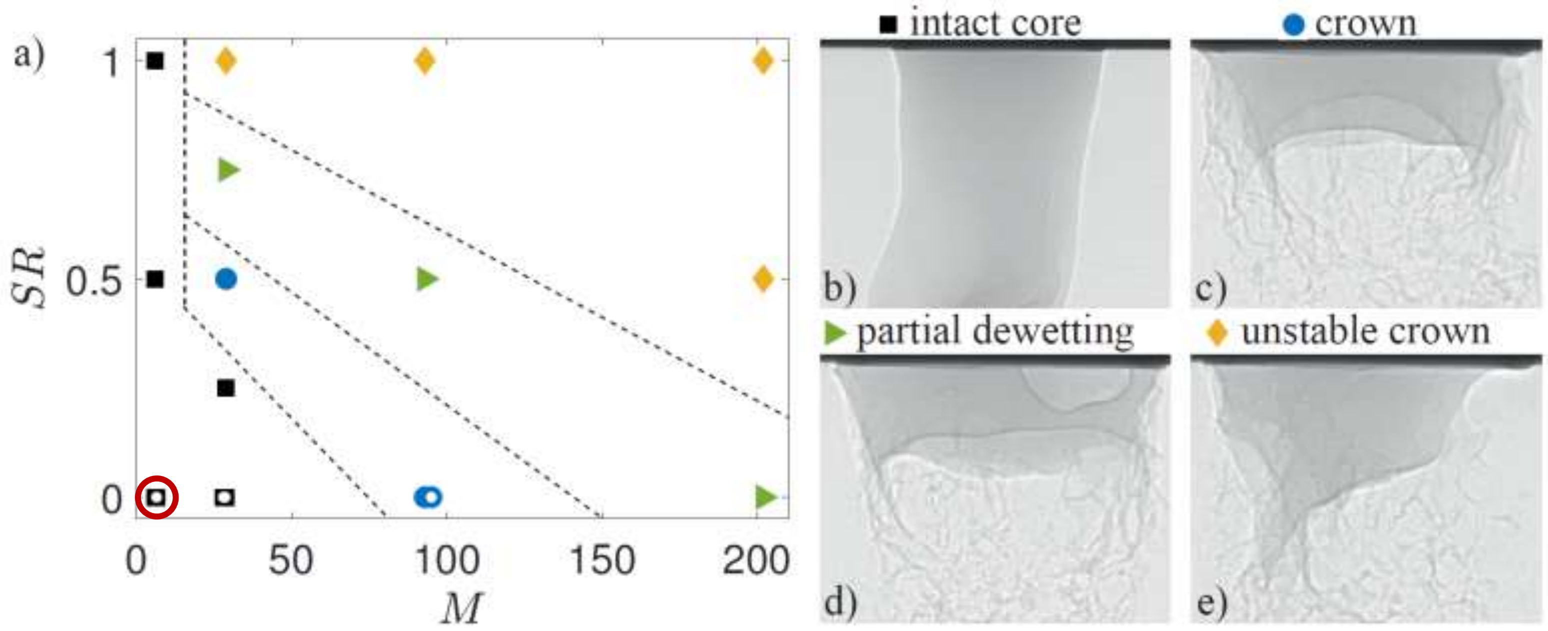

Stable and unstable liquid crown

$Re_l = 1100$ $We_g = 800$

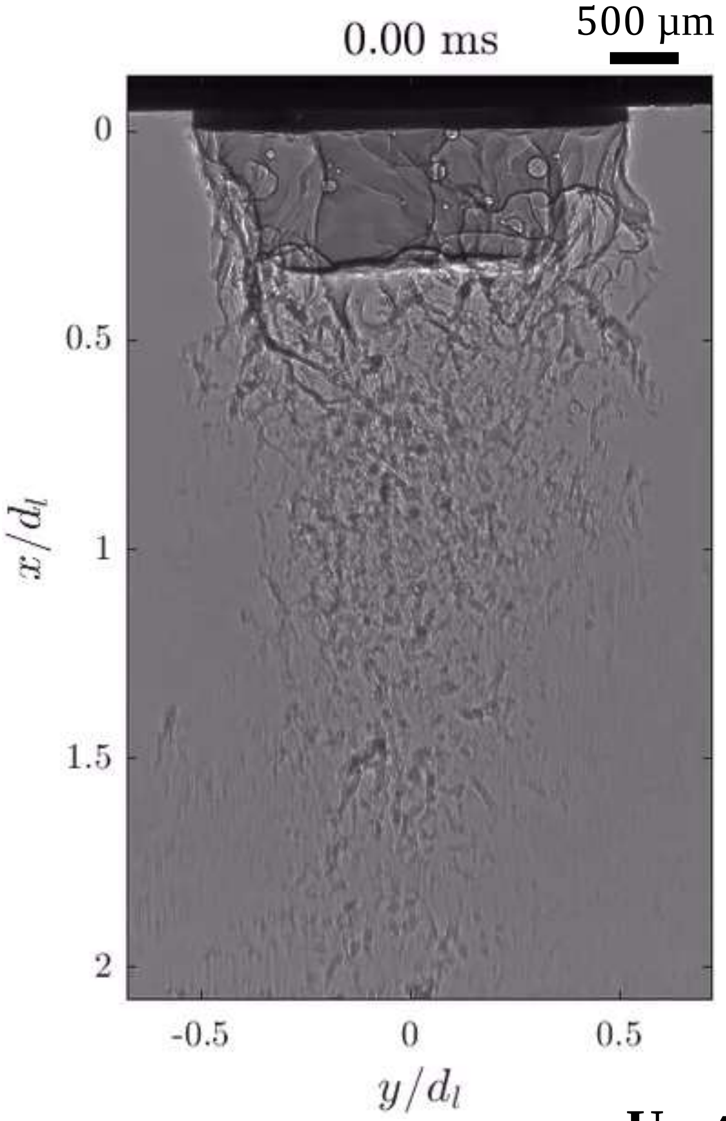

Machicoane et al., IJMF 2019

$Re_l = 1100, We_g = 1350$

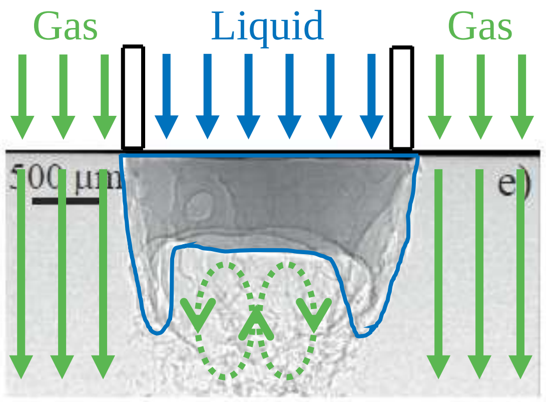

Crown

with gas swirl
➔ Unstable crown

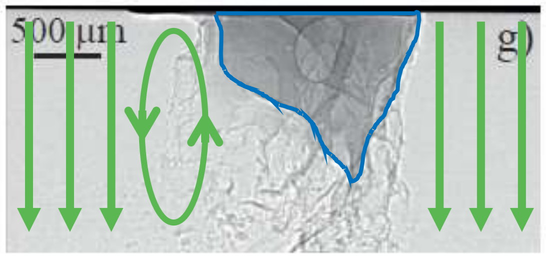

$Re_l = 800$ $We_g = 1100$

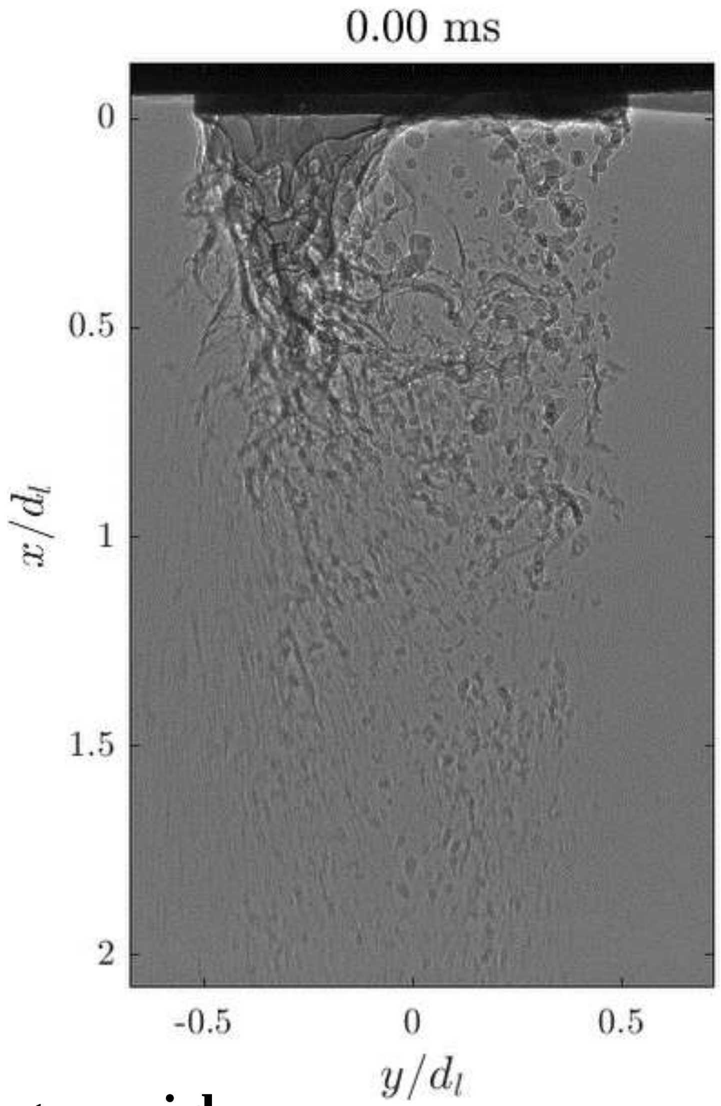

Unstable crown at extreme *M* values, without gas swirl

Visualization inside the liquid nozzle

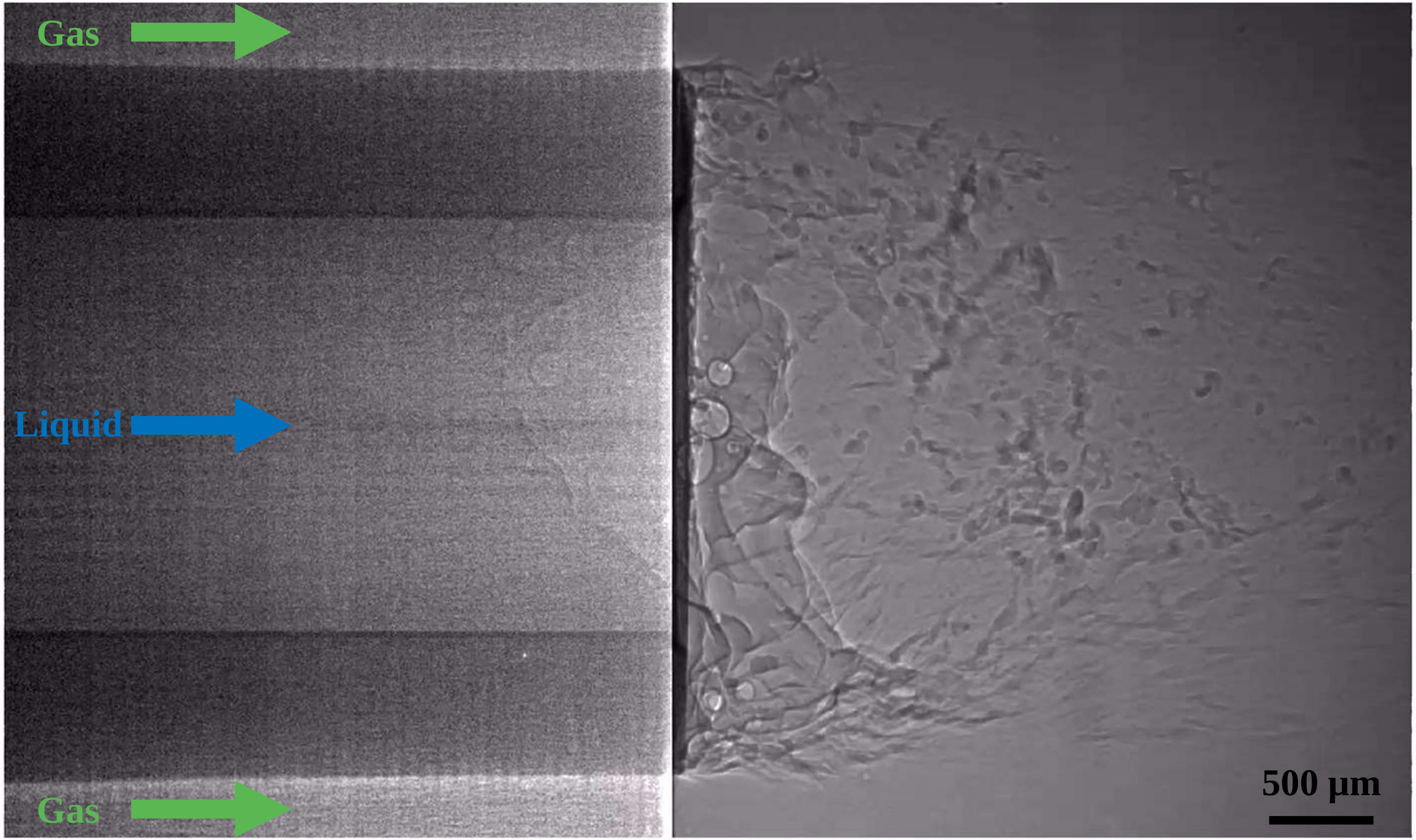

Transition between intact liquid core and crown

$Re_l = 3100$ $We_g = 800$

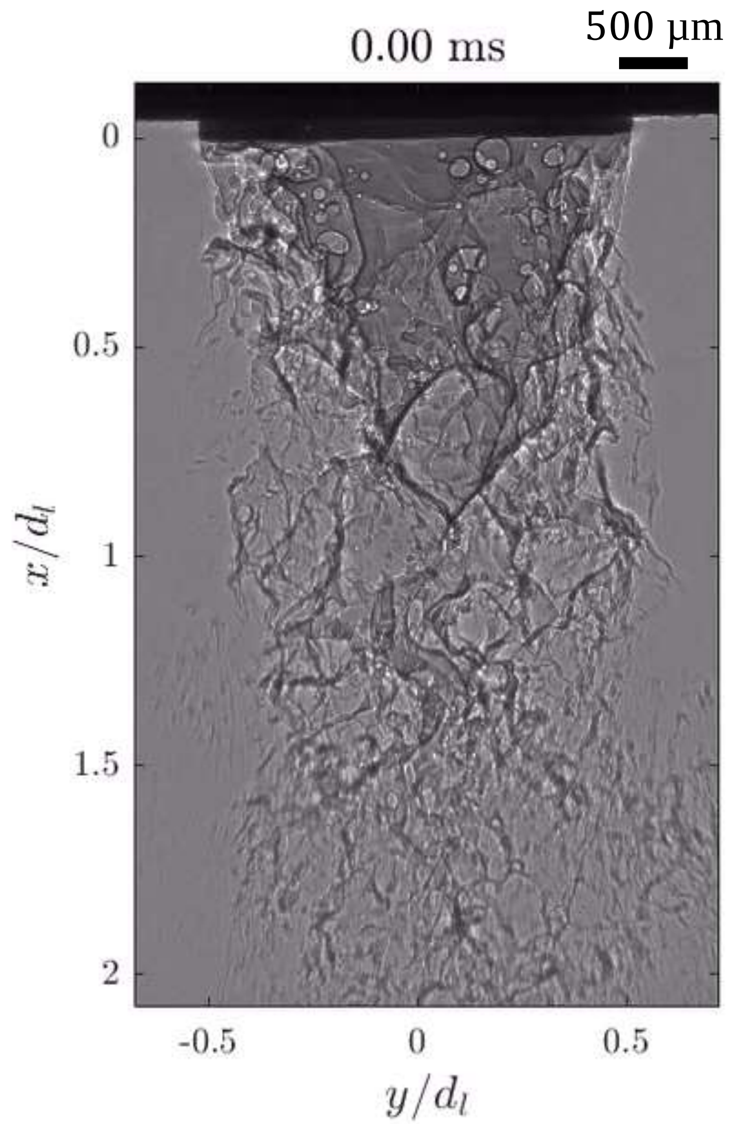

- Many overlapping interfaces
- Many smaller-scale gas recirculations
- « Perforated core » transition between intact core and crown

$$M = \frac{\rho_g u_g^2}{\rho_l u_l^2}$$

Kinetic energy arguments seem in good agreement for transition to crown and unstable crown

Intact core at $Re_l = 800$ $We_g = 45$

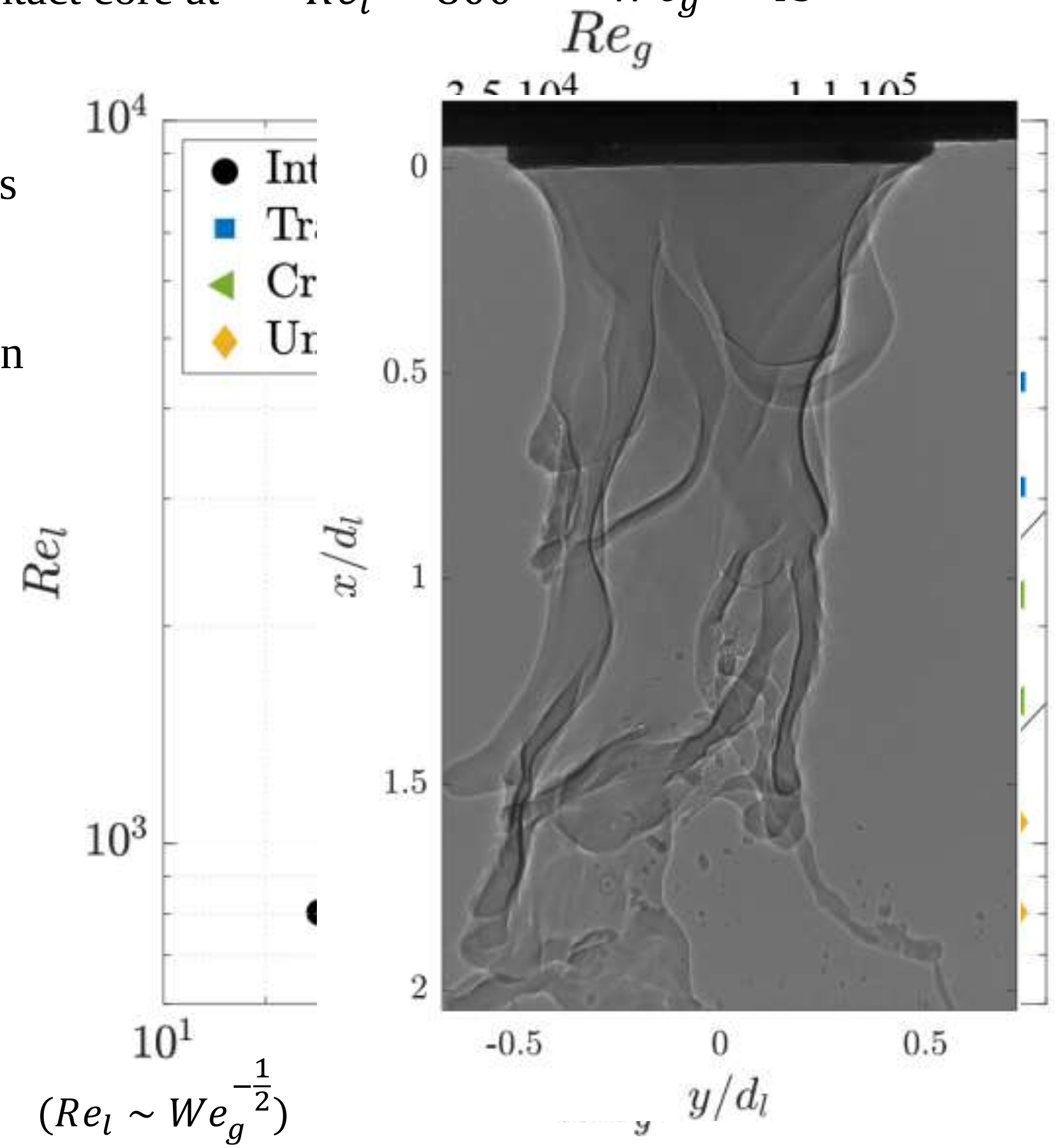

$(Re_l \sim We_g^{-\frac{1}{2}})$

Quantitative identification of unstable crown and role of swirl

X-ray absorption by the liquid jet follows Beer-Lambert's law

➔ Equivalent path length

using ANKA Phase
Weitkamp et al.
J. of Synchrotron
Radiation 2011

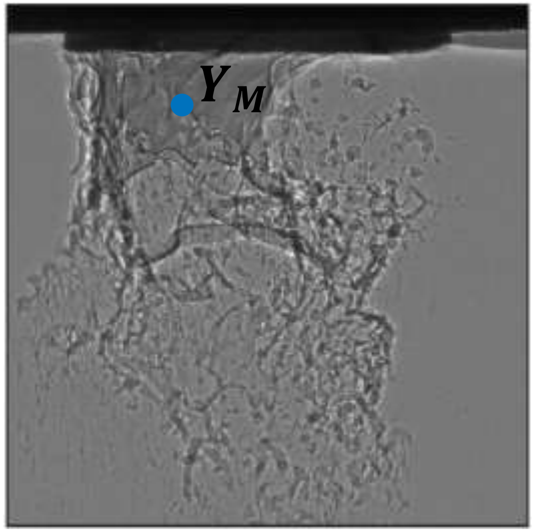

Center of mass along y

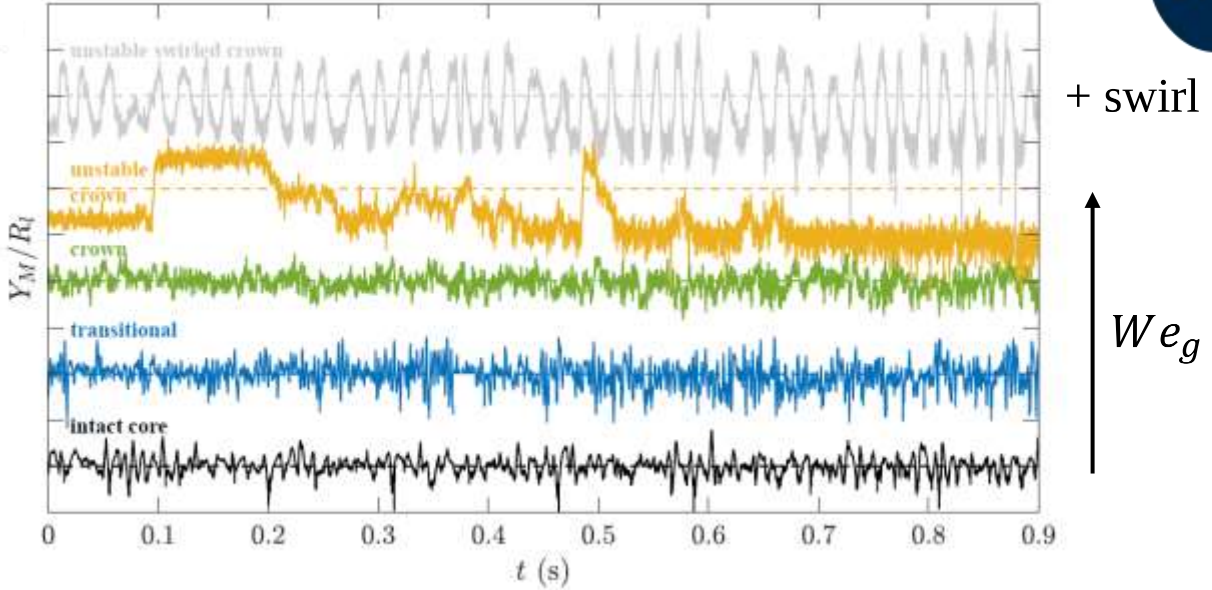

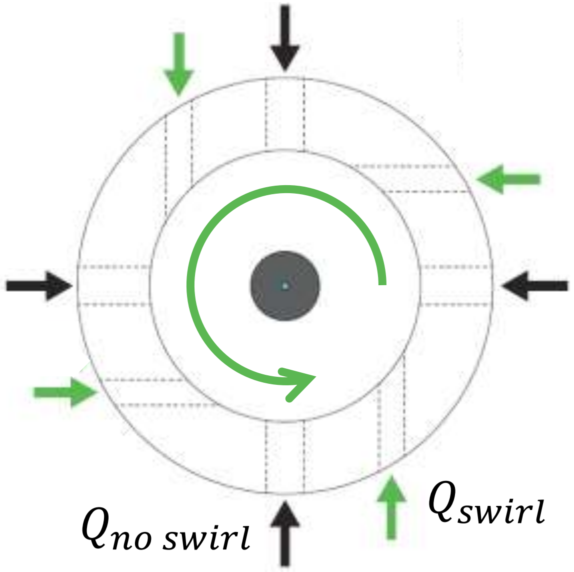

$$Q_{Total} = Q_{SW} + Q_{NS} = cst$$

$$SR = \frac{Q_{swirl}}{Q_{no\ swirl}}$$

$$Re_l = 800$$

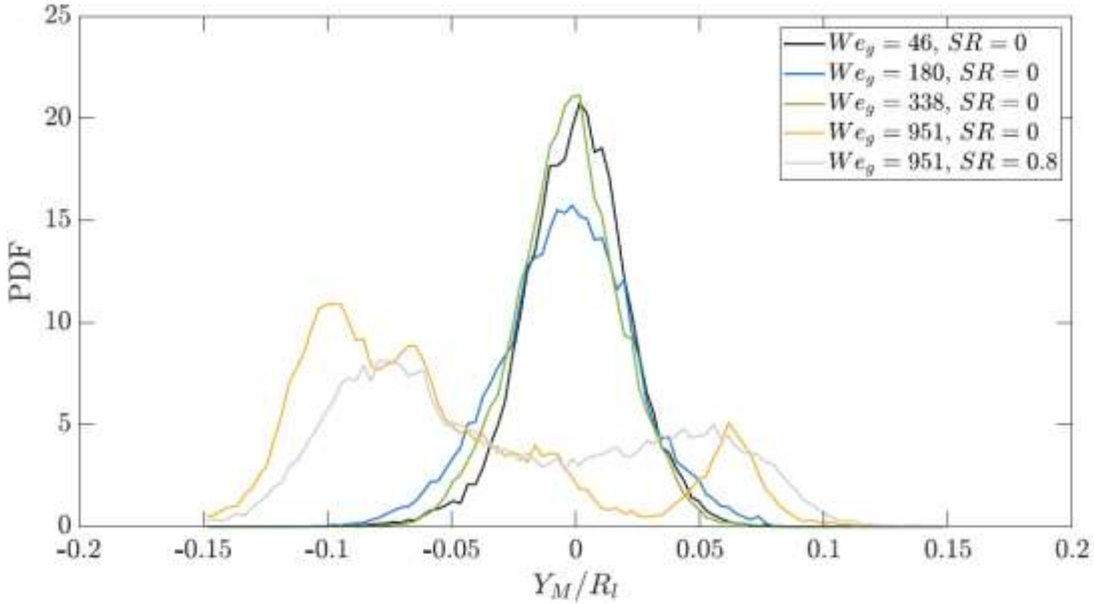

Quantitative identification of unstable crown and role of swirl

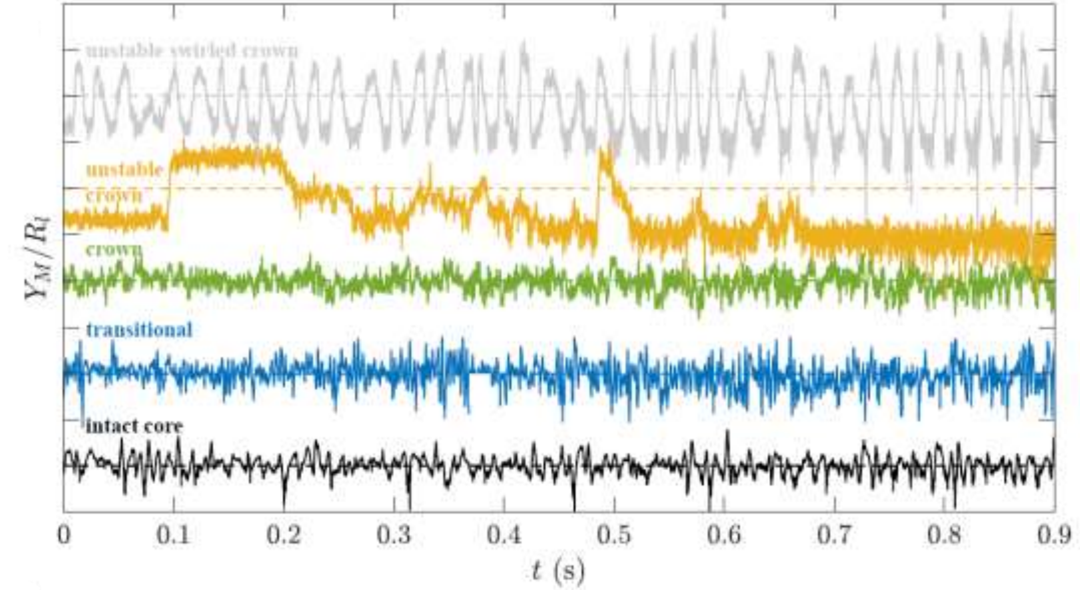

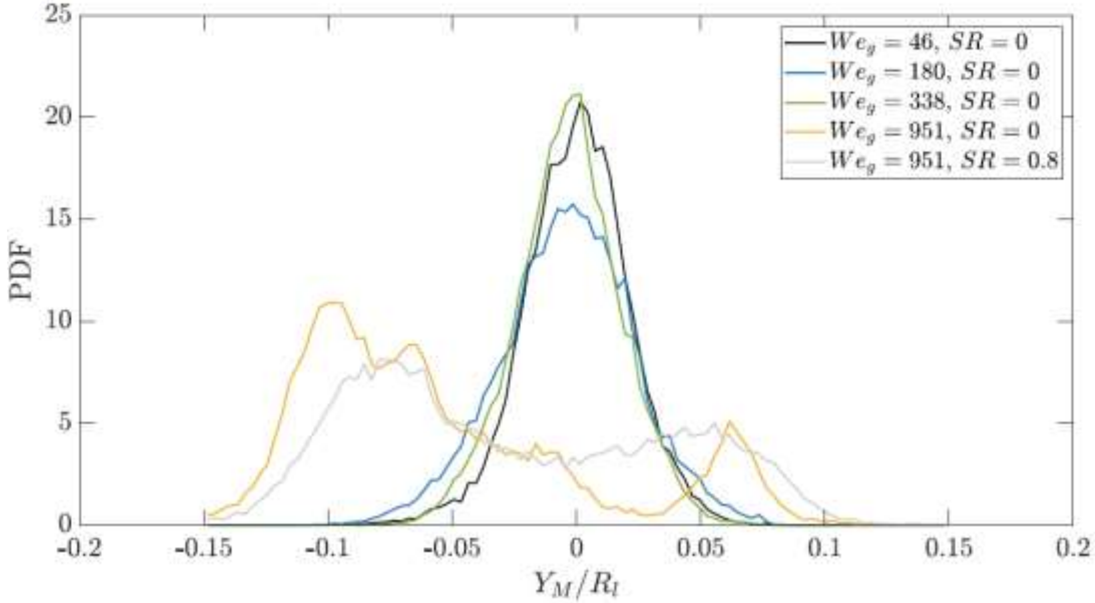

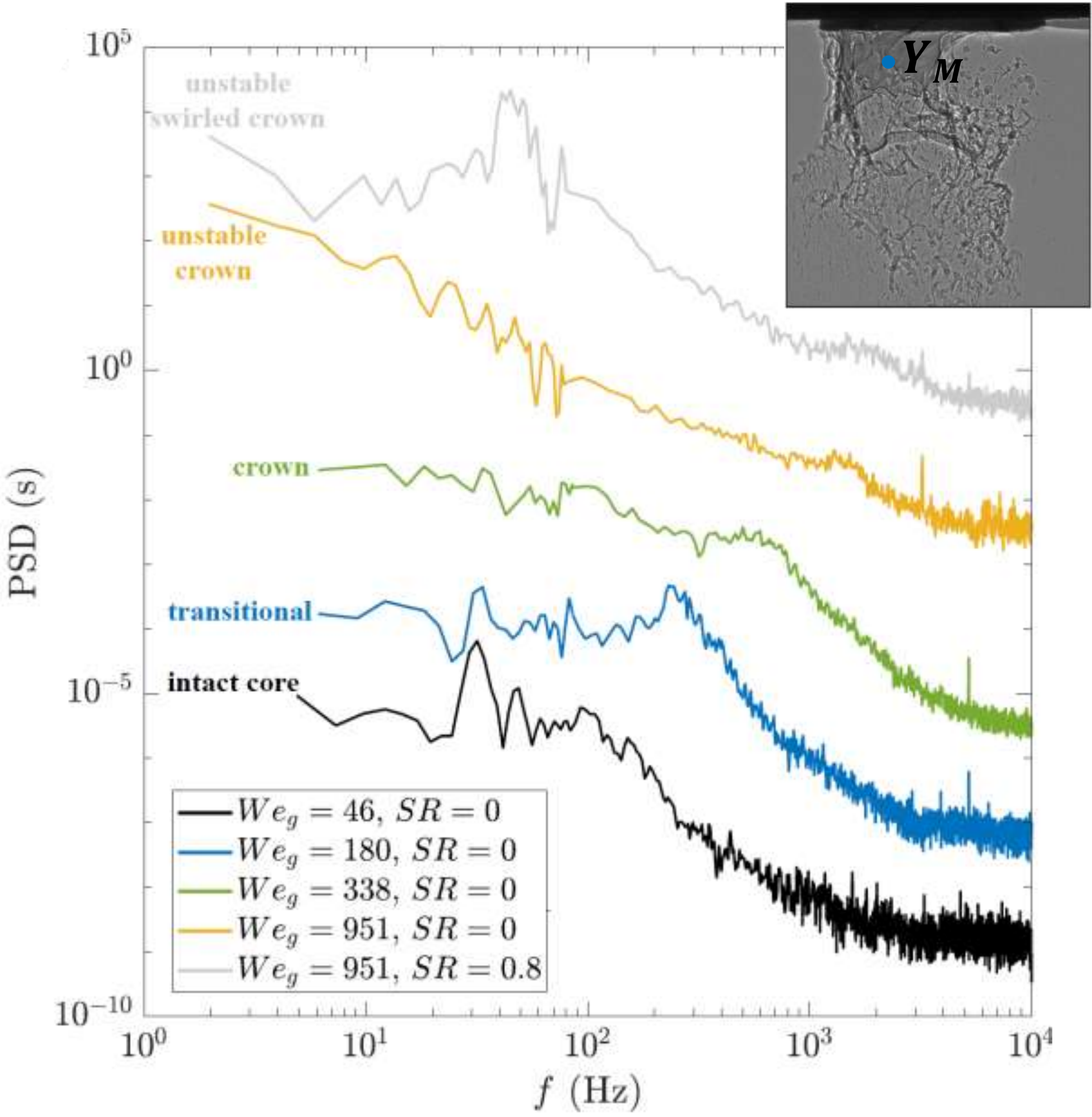

Flapping frequency

$$St = f d_g / U_g$$

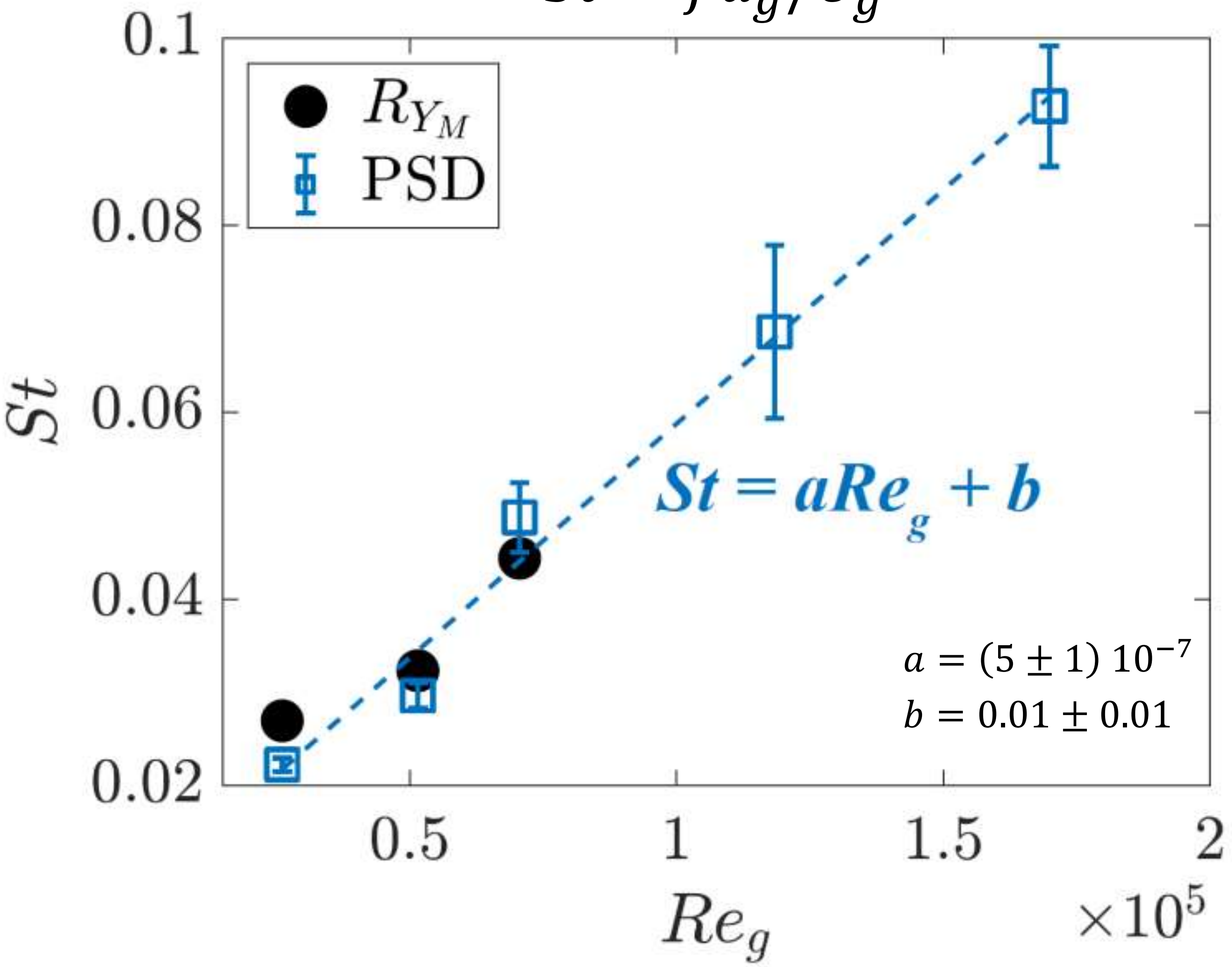

$St = aRe_g + b$

$a = (5 \pm 1)\, 10^{-7}$

$b = 0.01 \pm 0.01$

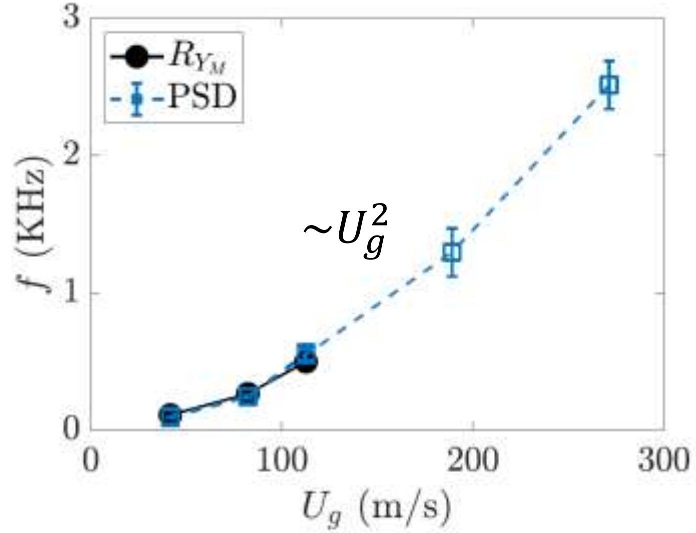

$\sim U_g^2$

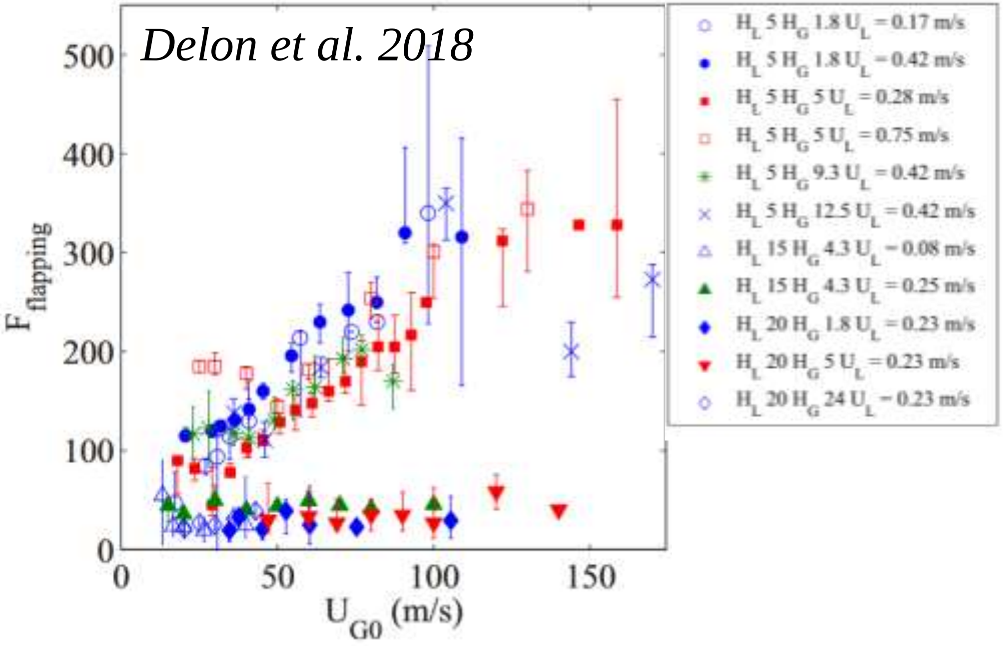

Delon et al. 2018

General conclusion

- At higher We_g, liquid core undergoes transitions, up to unstable crown, even without gas swirl
- Changes in atomization regimes and liquid core morphologies are entangled
- Gas swirl leads to earlier onset of unstable crown and much more frequent motions of the gas recirculation
- Study other mechanisms (e.g., flapping and instabilities) with swirl to try and relate to droplet size distributions

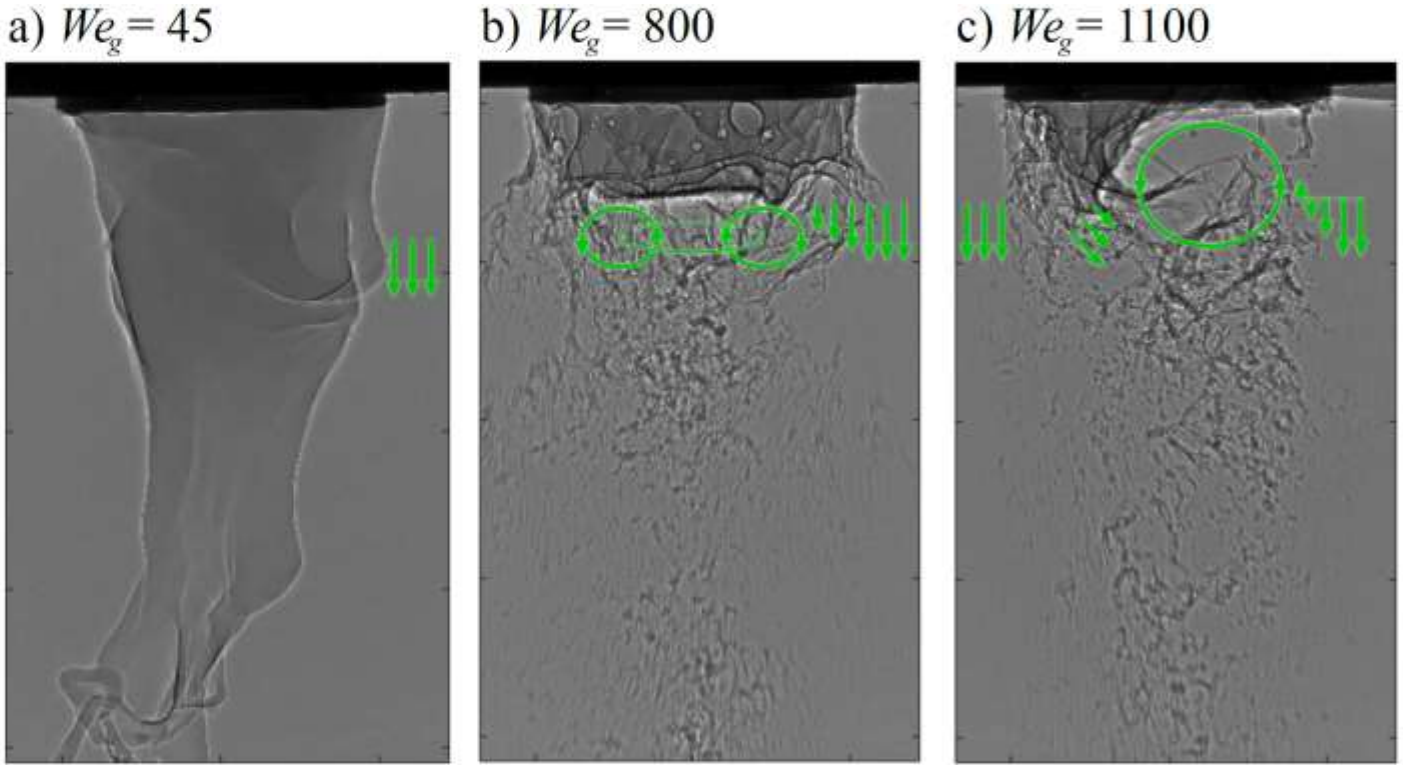

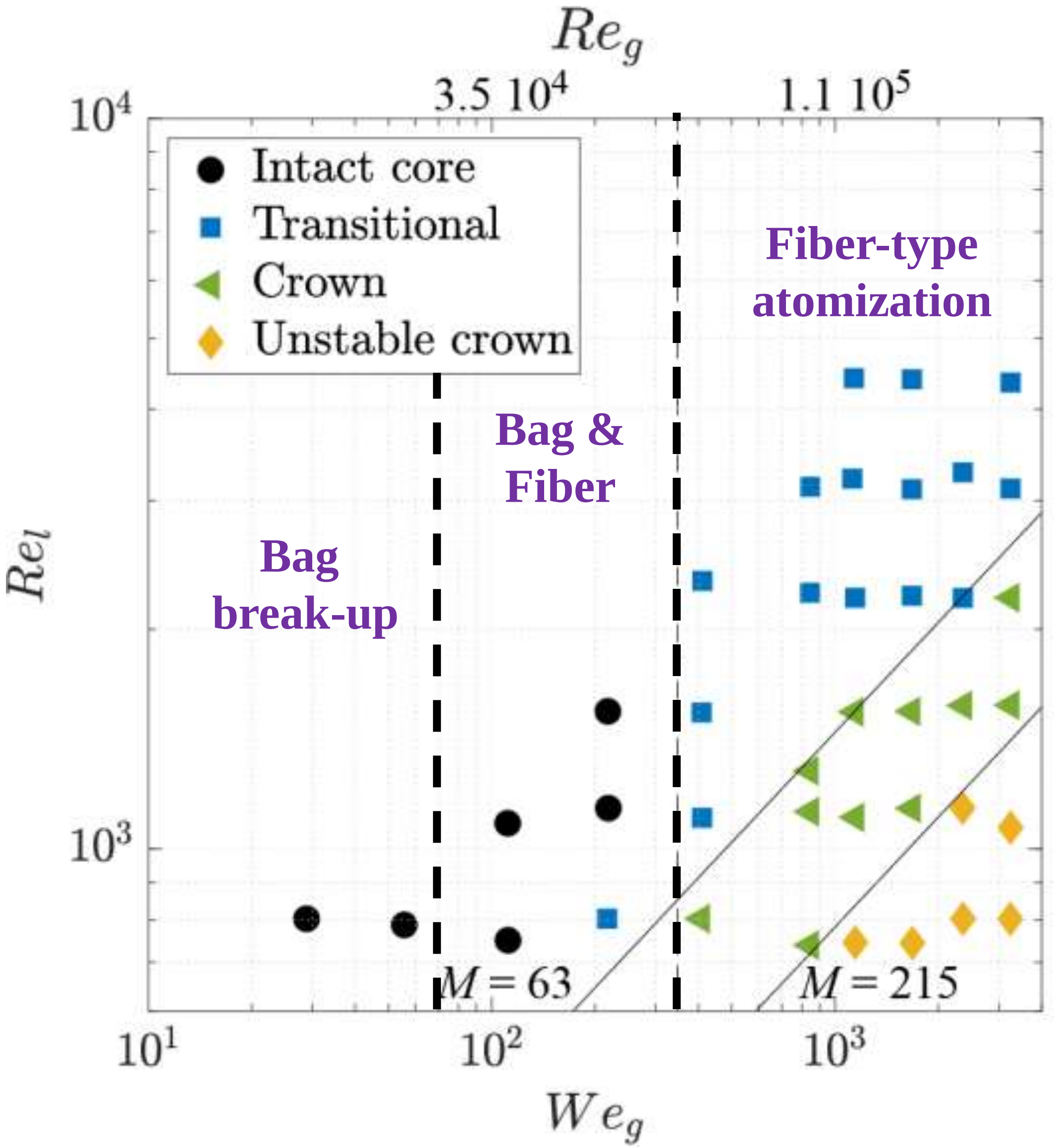

Thank you for your attention

February 10-14, 2025

Winter school NCTR VII

New Challenges in Turbulence Research

cnrs

UGA Université Grenoble Alpes

cea

ENS DE LYON

ÉCOLE DE PHYSIQUE DES HOUCHES

Relative Weber number

Based on slip velocity $We_r = \frac{\rho_g (u_g - u_l)^2 d_l}{\sigma}$

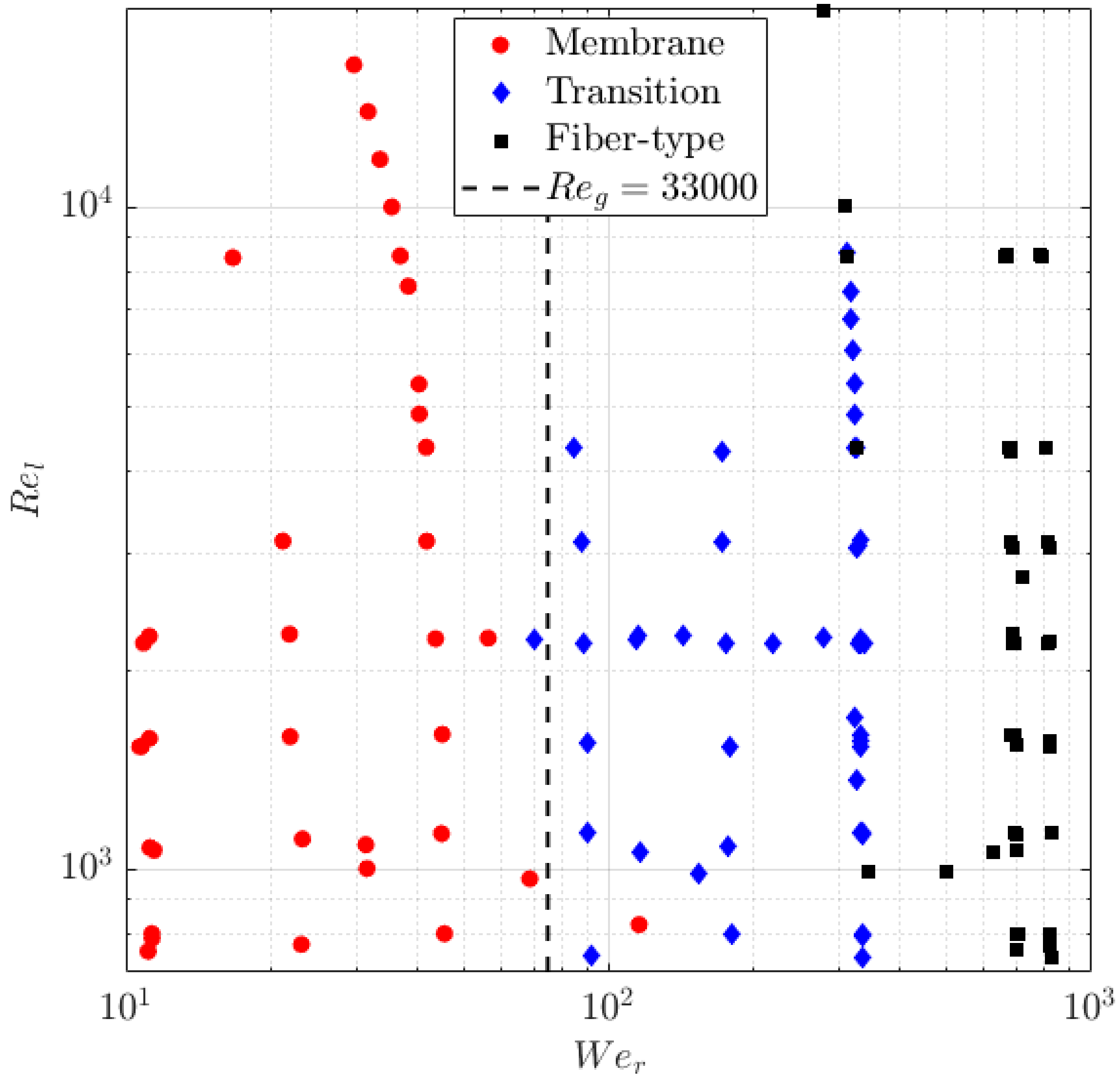

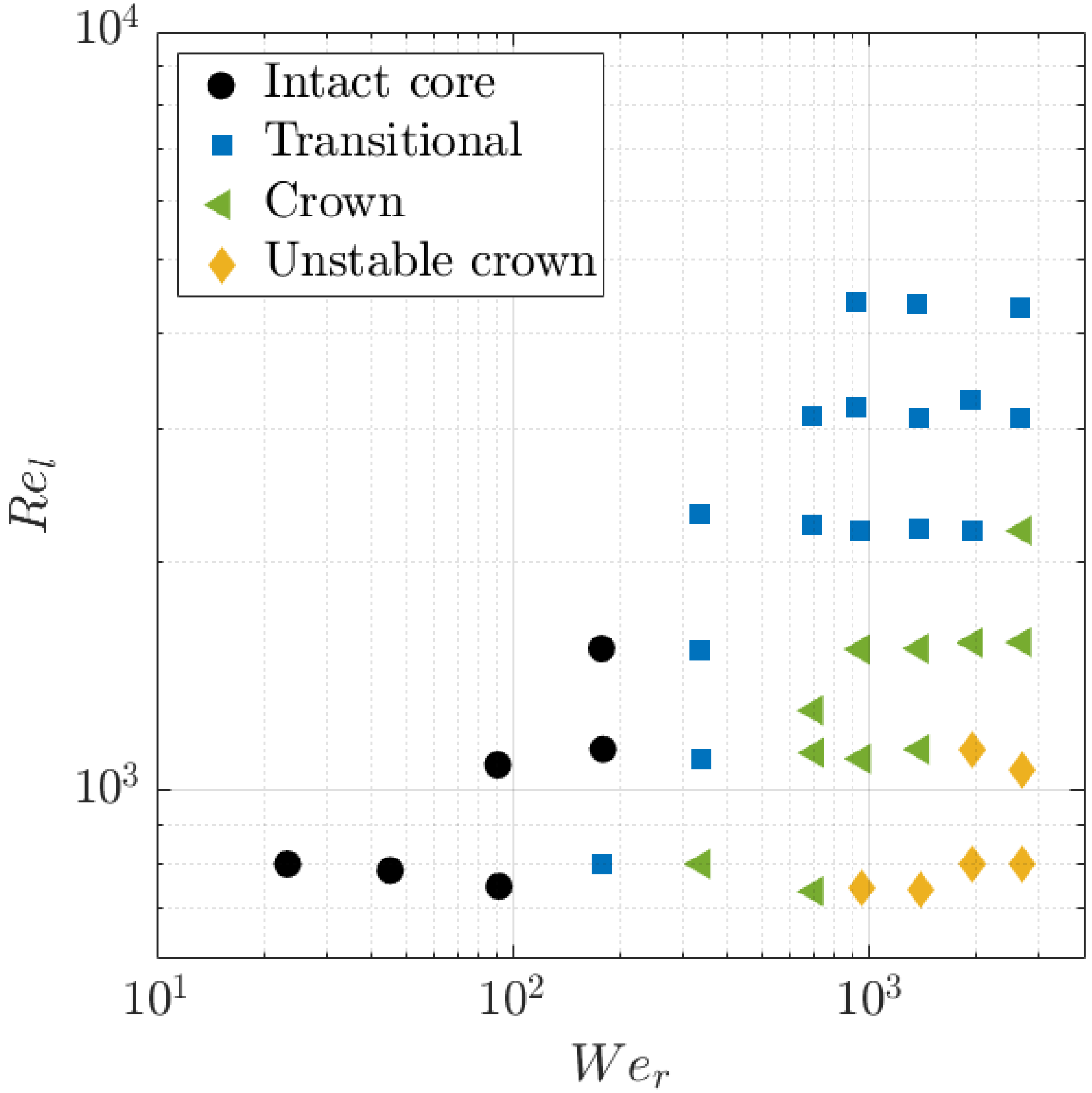

Spectra Ym

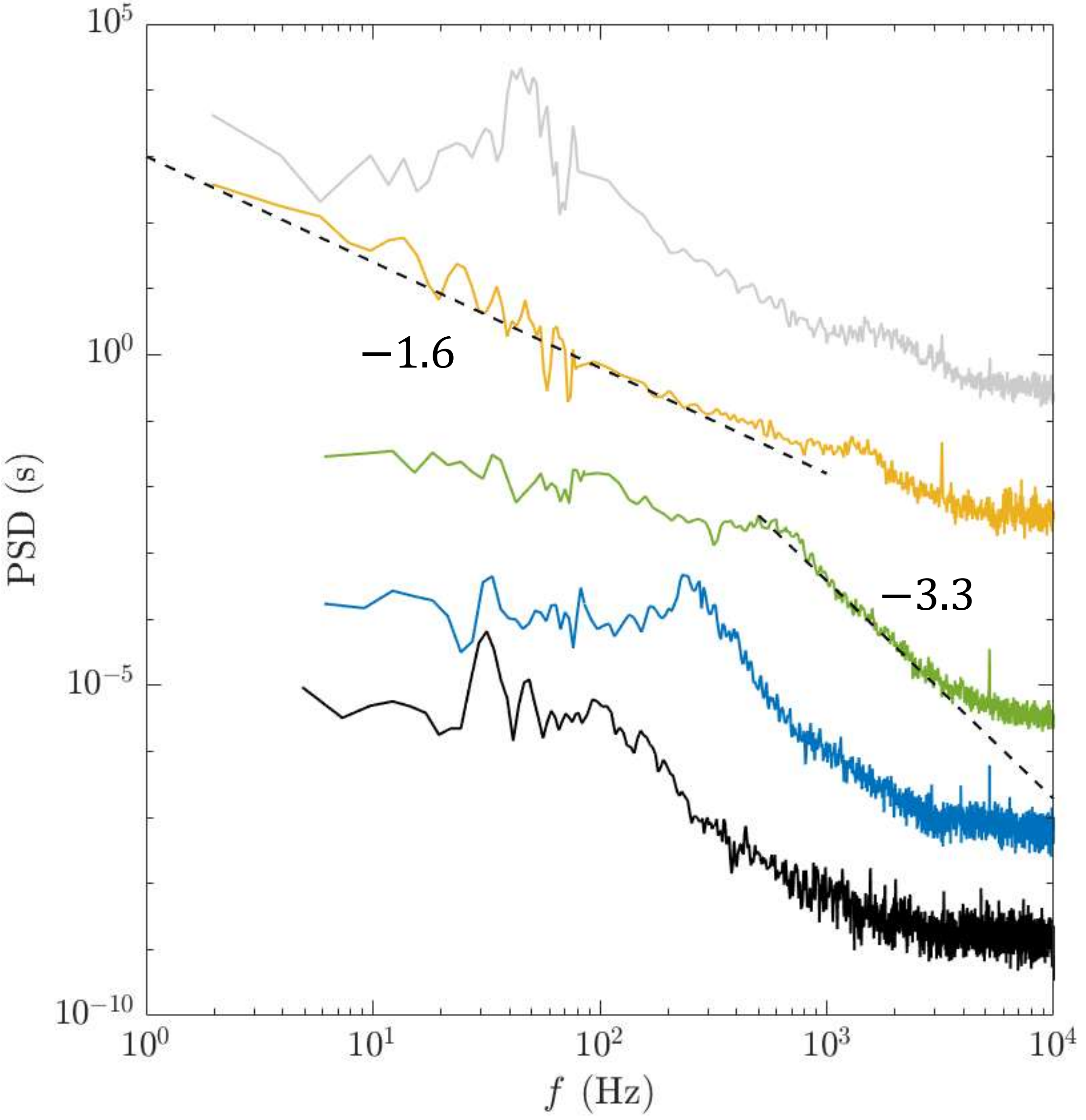
10^5
10^0
10^{-5}
10^{-10}
PSD (s)
-1.6
-3.3
10^0
10^1
10^2
10^3
10^4
f (Hz)

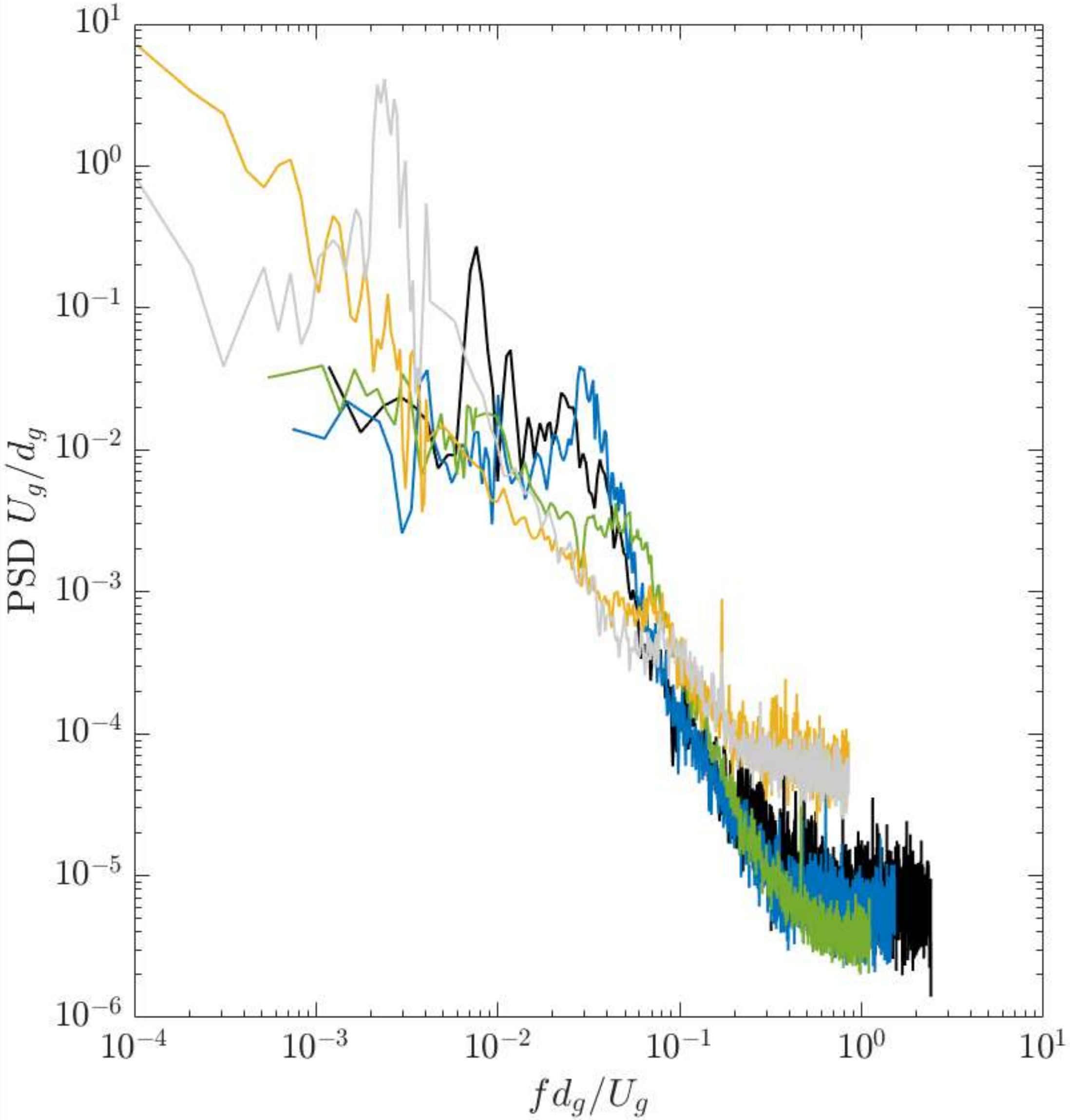
10^1
10^0
10^{-1}
10^{-2}
10^{-3}
10^{-4}
10^{-5}
10^{-6}
PSD U_g/d_g
10^{-4}
10^{-3}
10^{-2}
10^{-1}
10^0
10^1
$f d_g/U_g$

Closer Look at X-ray $M = 80$

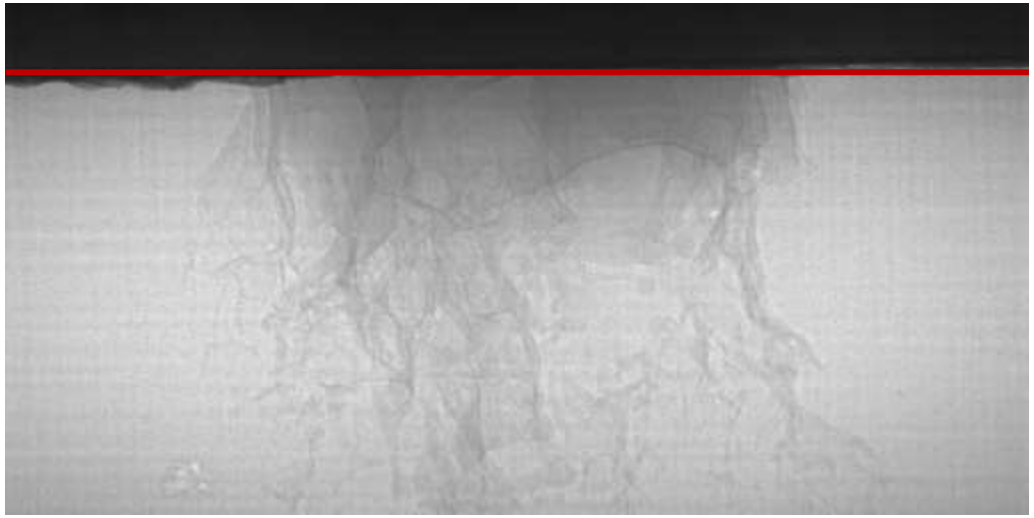

$x = 0$

$x = 0.21d_g$

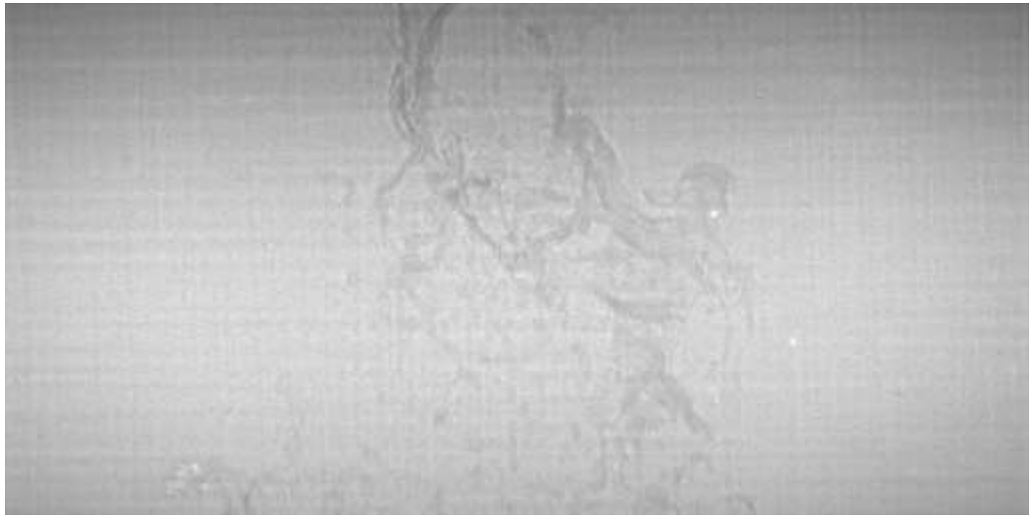

$x = 0.17d_g$

$x = 0.41d_g$

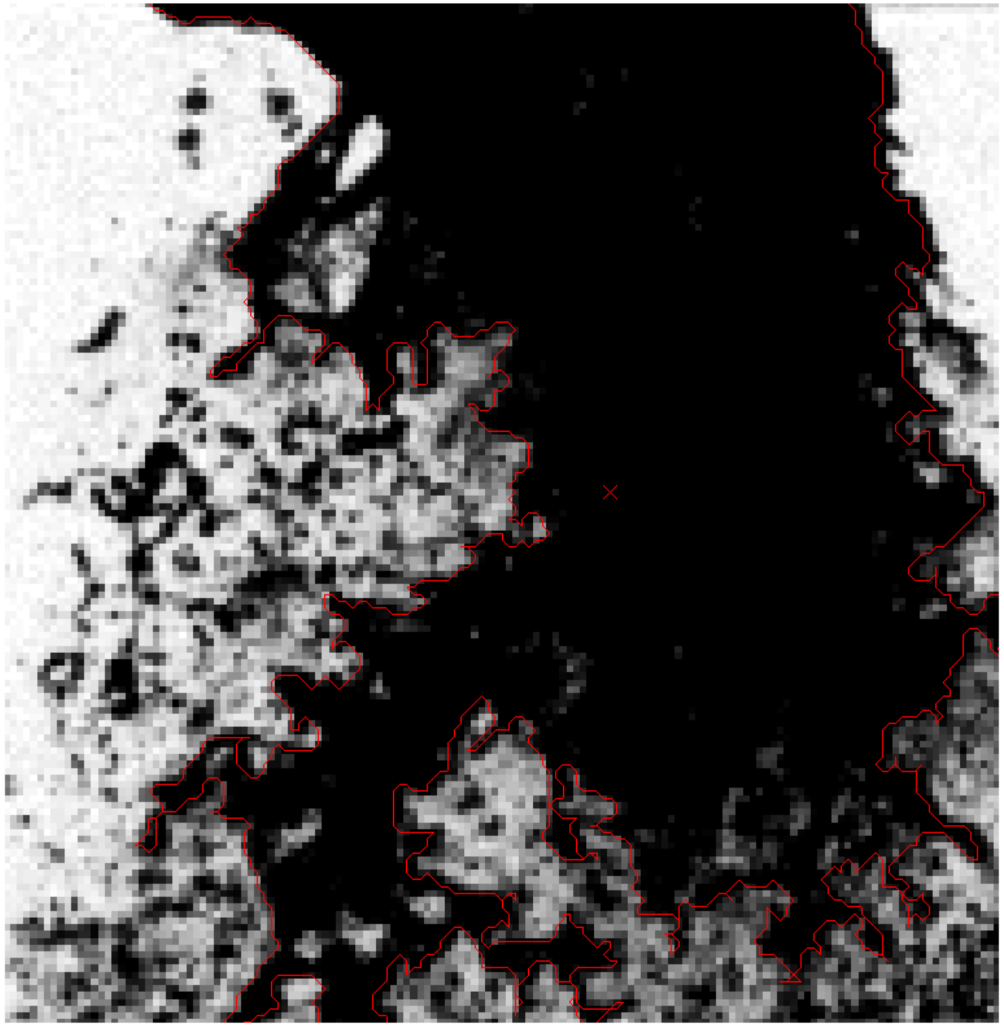

ANKA Phase: from intensity to liquid thickness

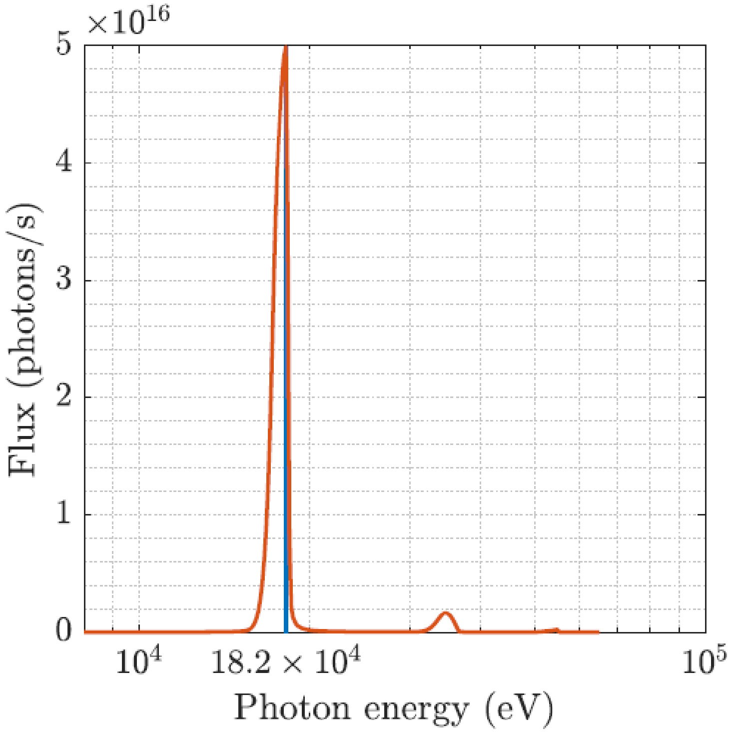

Incoming X-ray beam
energy spectrum

X-ray absorption by the liquid jet follows Beer-Lambert’s law

➔ Equivalent path lenght (EPL)

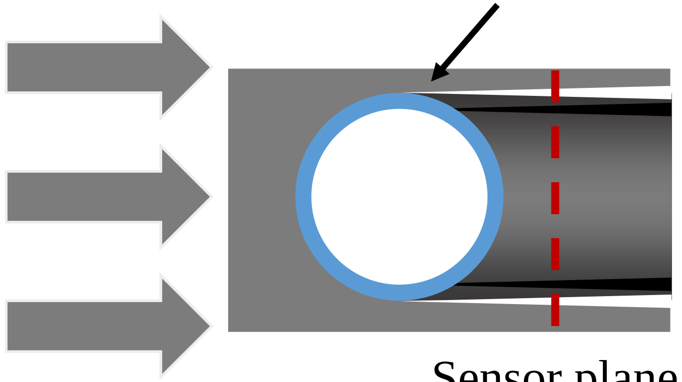

Interferences
(X-ray scatter by interfaces)

Sensor plane

I_0

$I(x, y, t)$

$$\frac{I(x,y,t)}{I_0(x,y)} = \int e^{-\mu(\lambda) h(x,y,t)} d\lambda$$

- Remove interferences $f(x, y, \lambda)$
- Retrieve phase map ϕ
- Convert into EPL map

Weitkamp et al.
J. of Synchrotron Radiation 2011

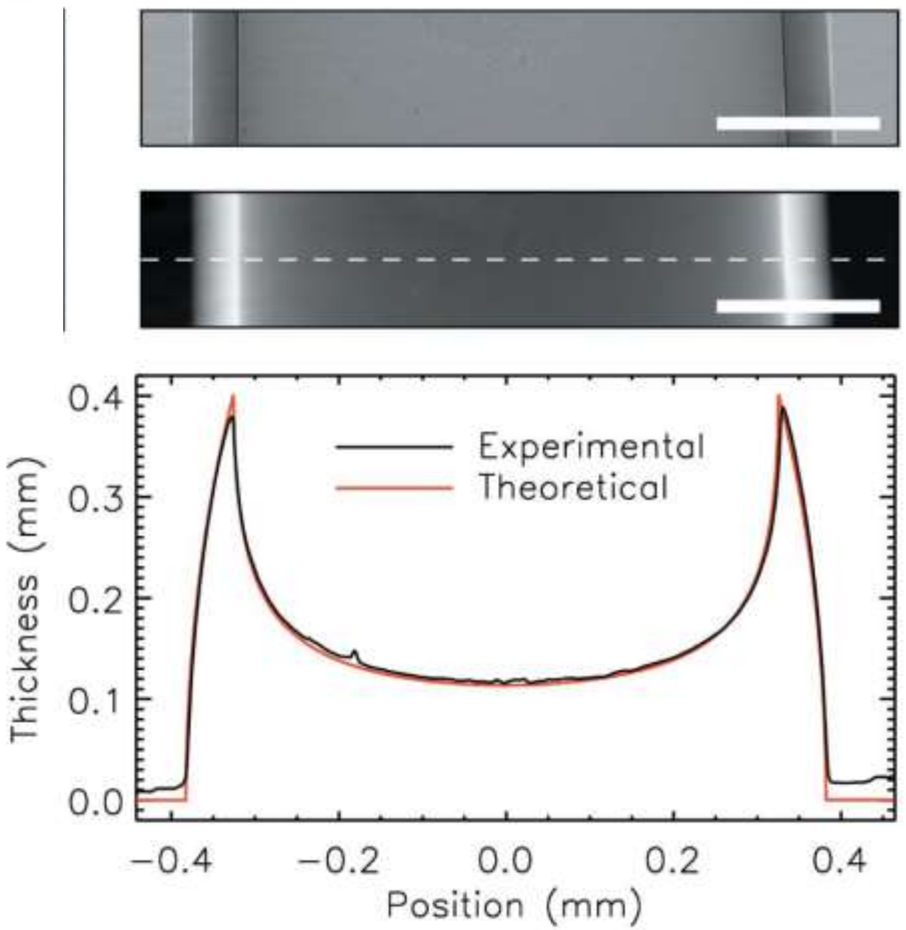

Normalized radiograph
Phase map
EPL

ANKA Phase: from intensity to liquid thickness

Weitkamp et al., J. of Synchrotron Radiation 2011

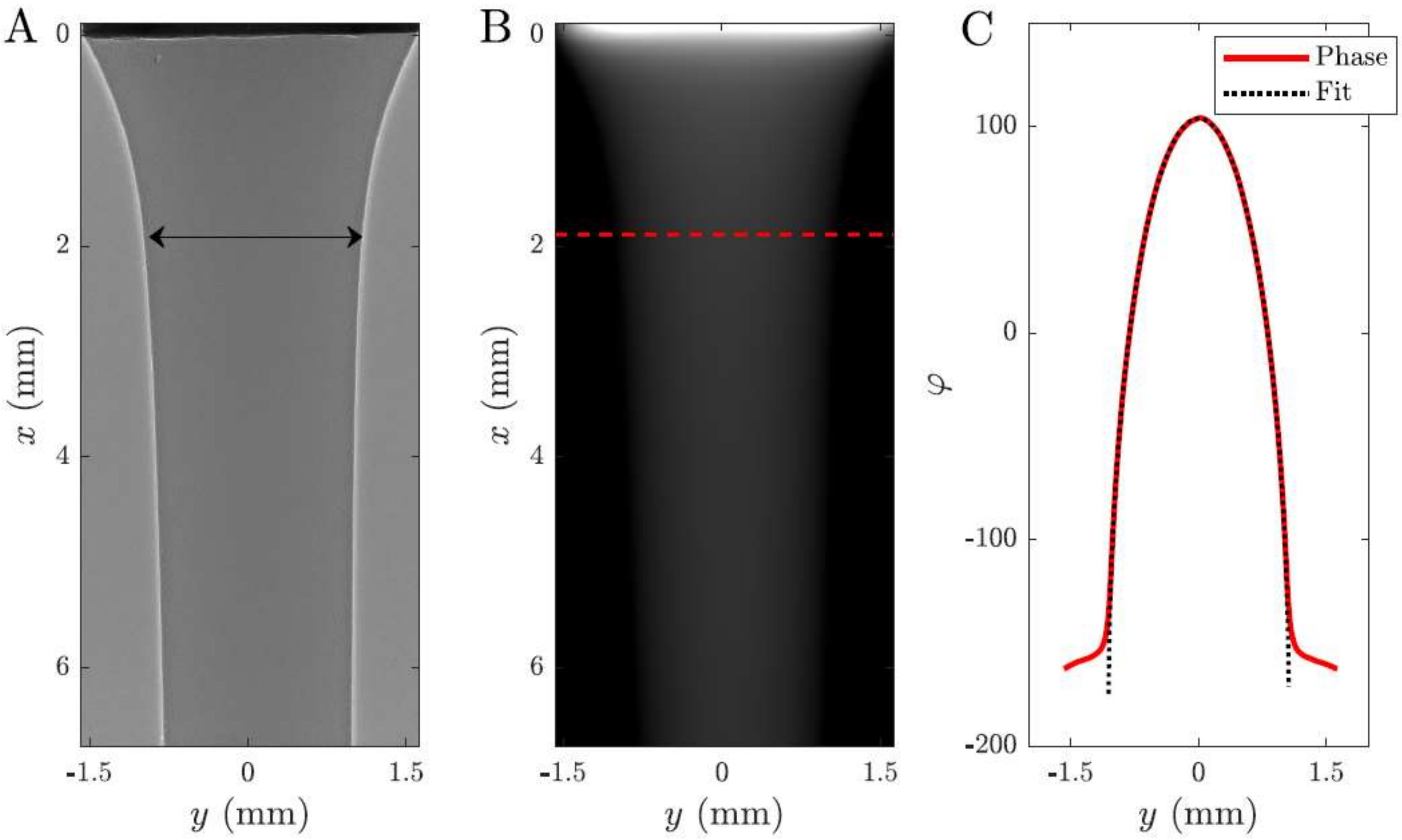

X-ray absorption by the liquid jet follows Beer-Lambert's law

➔ Equivalent path lenght (EPL)

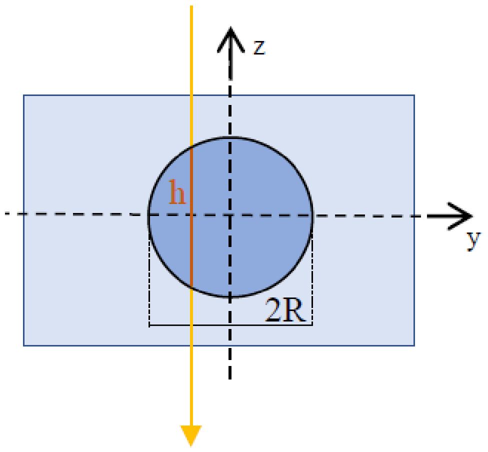

$$\phi = \alpha h(y) + \beta$$

$$h(y) = 2R\sqrt{1-(y/R)^2}$$

➔ Calibrate for the coefficient α and β (non-monochromatic, spatial and temporal inhomogeneities…)

Calibration of the phase maps conversion

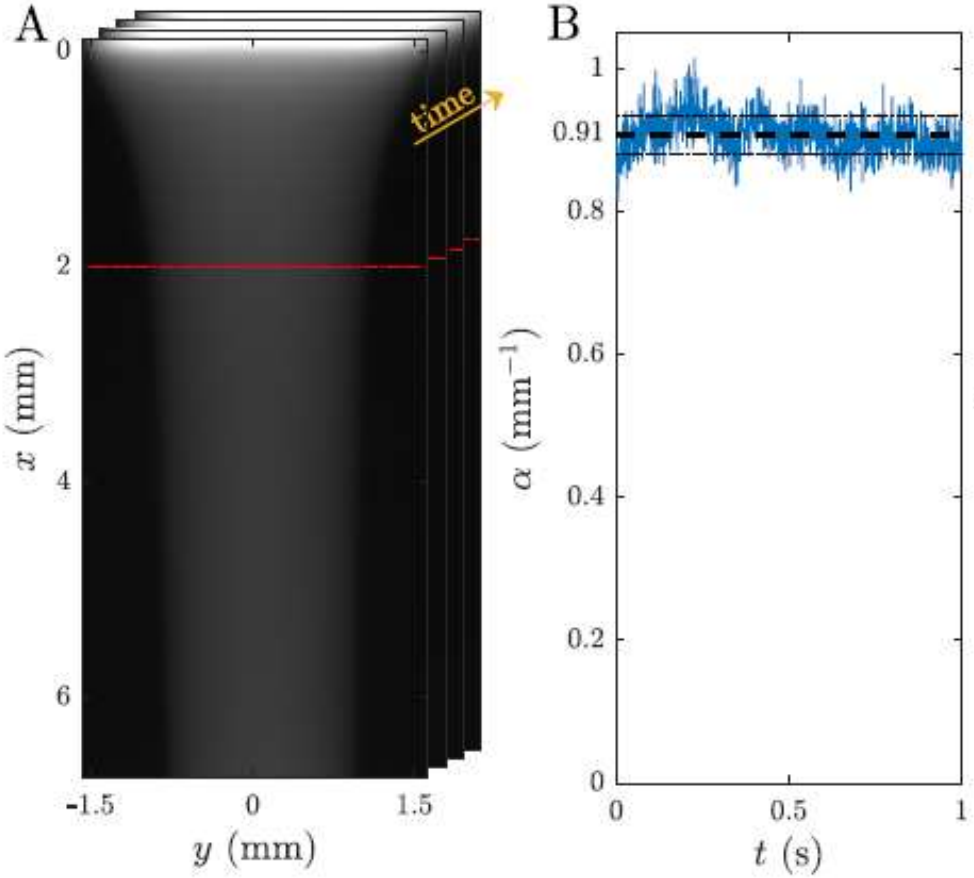

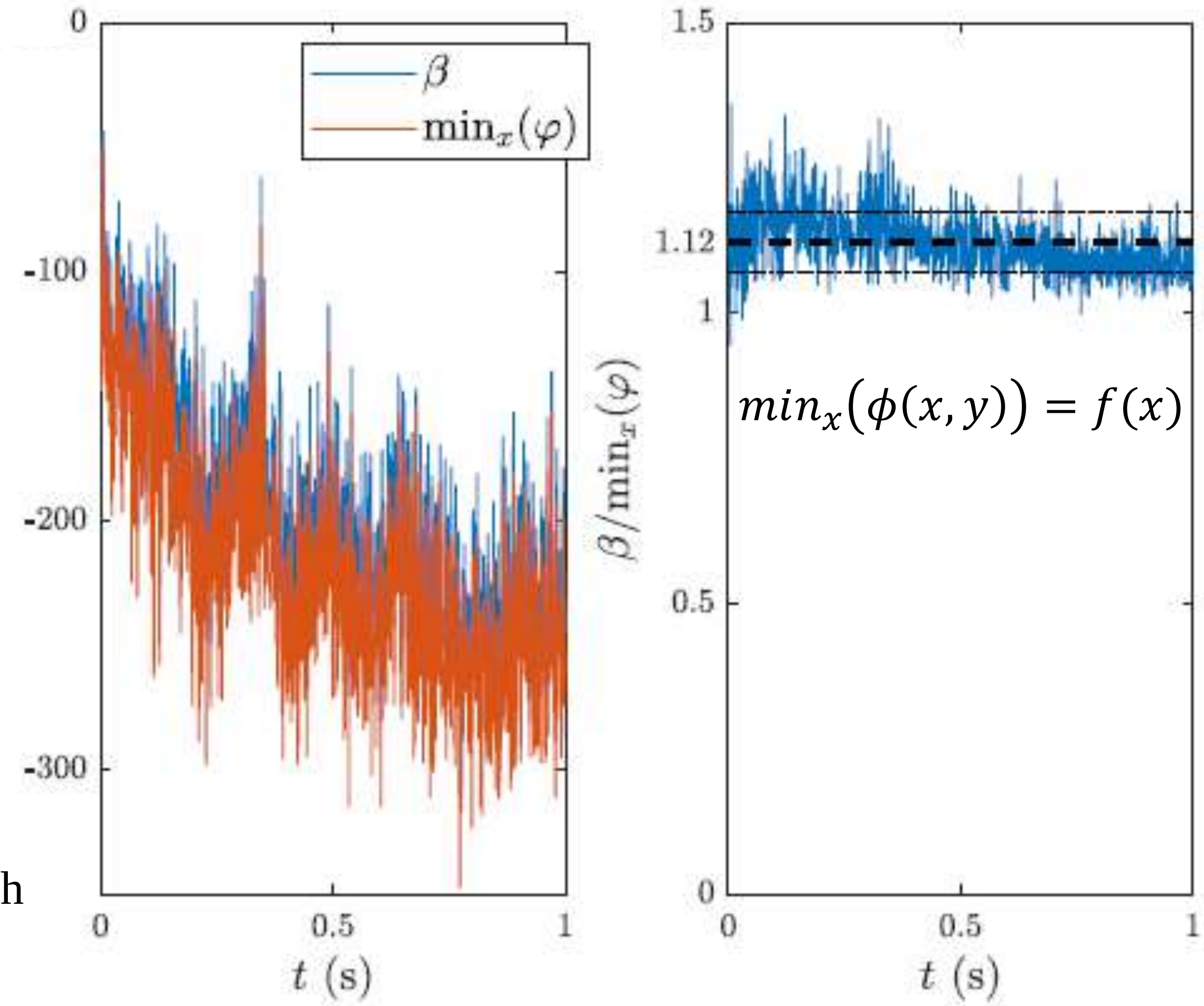

$min_x\big(\phi(x,y)\big) = f(x)$

α, β depend on the sample and on the X-ray wavelength

➔ $\alpha = 0.91\ \mathrm{mm}^{-1}$ and $\beta = 1.12\, min_x(\phi)$ for what follows

Measurement uncertainties

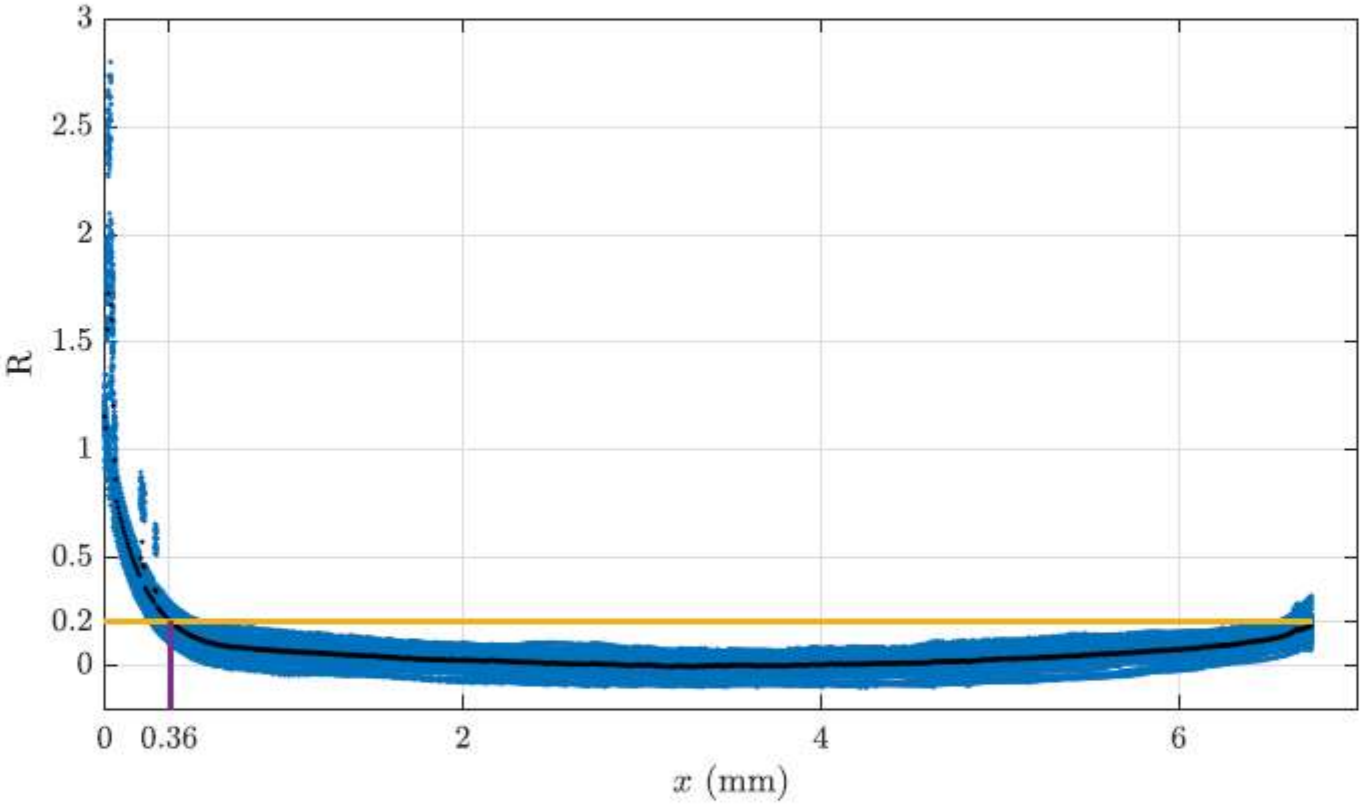

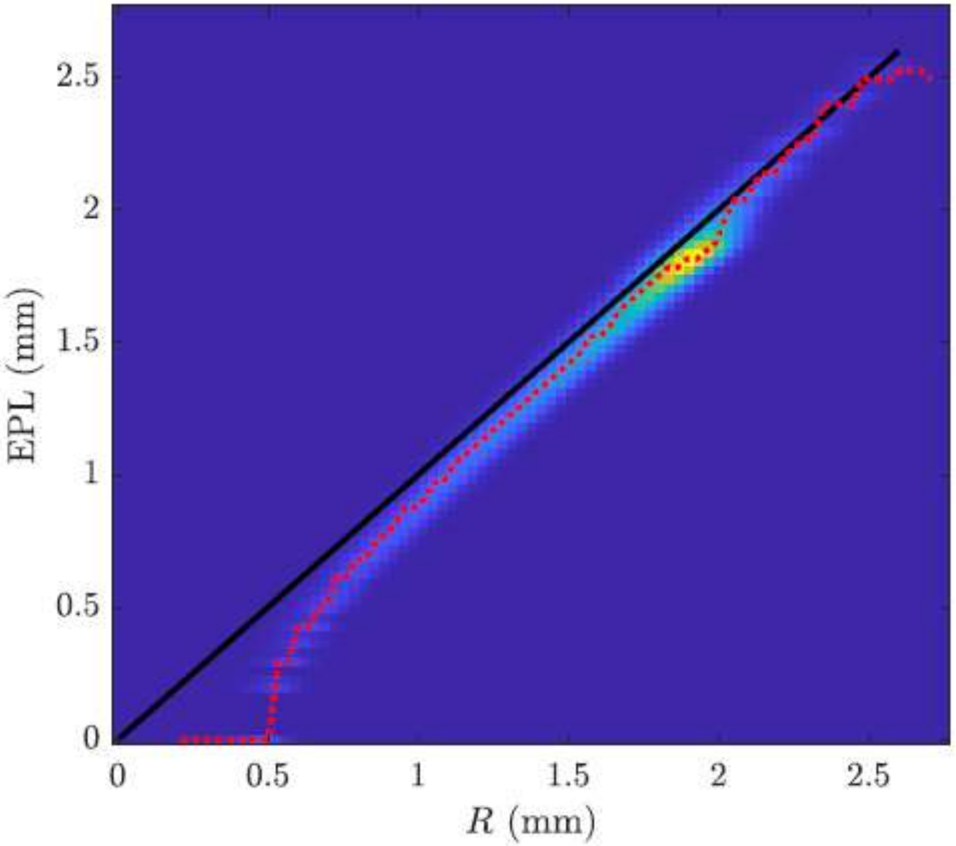

Longitudinal cut along the liquid jet

2D PDF: EPL vs fitted radii

Limitations of the uncertainties' evaluation

- Nozzle glare (ANKA Phase is for a single material)
- Interference patterns due to X-ray scattering by interfaces limit the probing of small radius values

➔ For $x > \frac{D_l}{10}$ and for $EPL > 1$ mm, approximately 10% accuracy (~ 20% for smaller thicknesses?)

X-ray energy spectrum

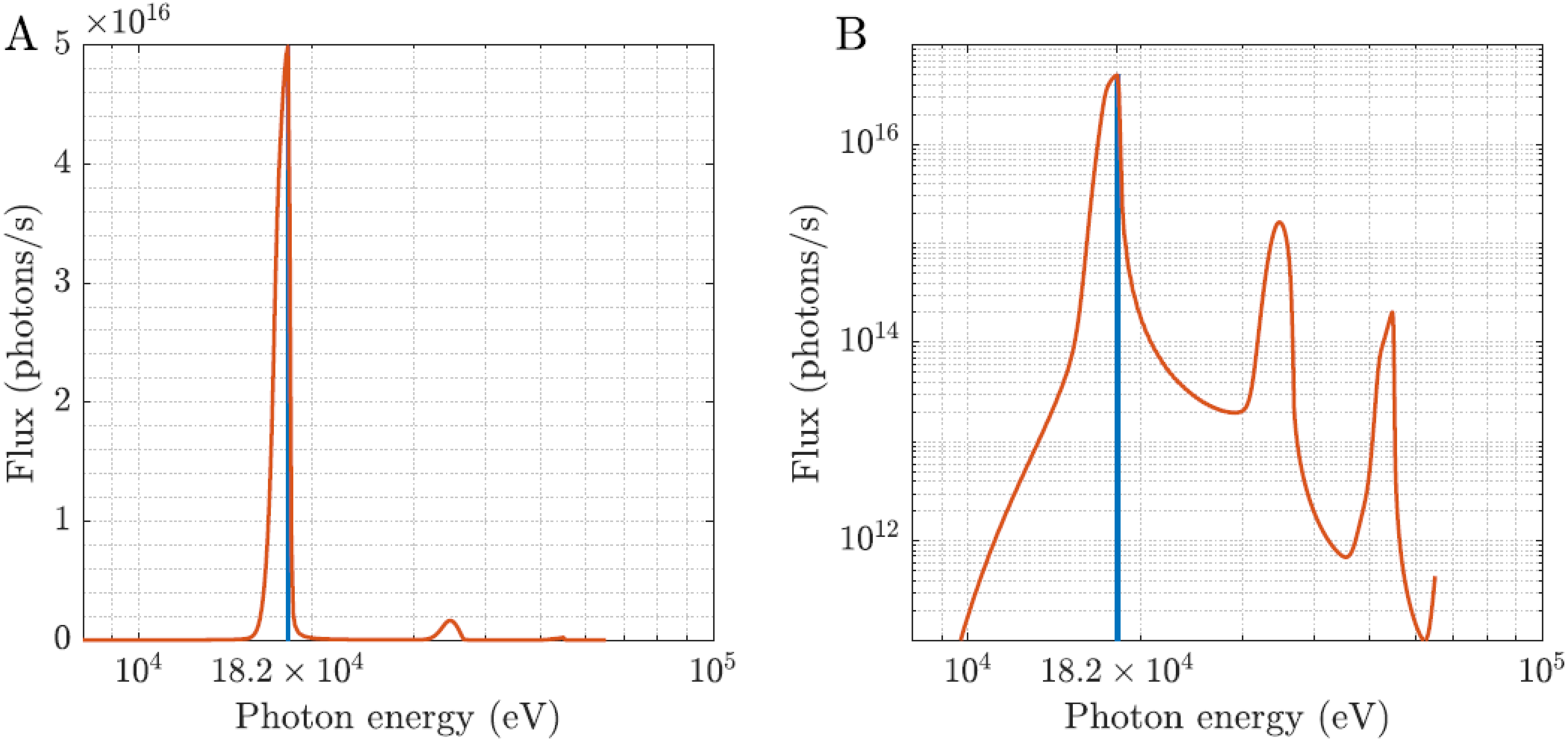

High-speed spray flapping

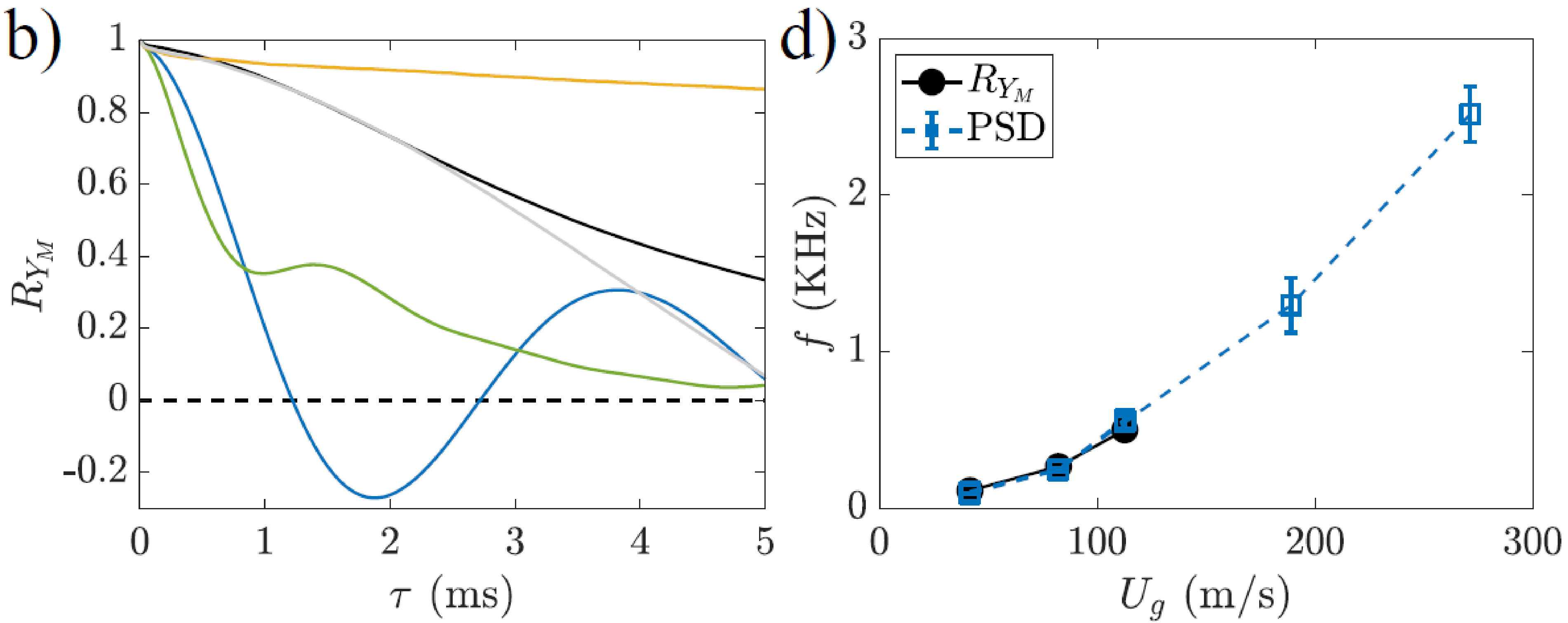

High-speed spray Slopes on power spectra